COMMUN. MATH. SCI.
Vol. 15, No. 3, pp. 813–837
© 2017 International Press

A ROBUST HIGH-ORDER DISCONTINUOUS GALERKIN METHOD WITH LARGE TIME STEPS FOR THE COMPRESSIBLE EULER EQUATIONS*

FLORENT RENAC†

Abstract. We present a high-order Lagrange-projection like method for the approximation of the compressible Euler equations with a general equation of state. We extend the method introduced in Renac [F. Renac, Numer. Math., 2016, DOI 10.1007/s00211-016-0807-0] in the case of the isentropic gas dynamics to the compressible Euler equations and minimize the numerical dissipation by quantifying it from a parameter evaluated locally in each element of the mesh. The method is based on a decomposition between acoustic and transport operators associated to an implicit-explicit time integration, thus relaxing the constraint of acoustic waves on the time step as proposed in Coquel *et al.* [F. Coquel, Q. Long-Nguyen, M. Postel and Q.H. Tran, Math. Comput., 79:1493–1533, 2010] in the context of a first-order finite volume method. We derive conditions on the time step and on a local numerical dissipation parameter to keep positivity of the mean value of the discrete density and internal energy in each element of the mesh and to satisfy a discrete inequality for the physical entropy at any approximation order in space. These results are then used to design limiting procedures in order to restore these properties at nodal values within elements. Moreover, the scheme is designed to avoid over-resolution in space and time in the low Mach number regime. Numerical experiments support the conclusions of the analysis and highlight stability and robustness of the present method when applied to either discontinuous flows or vacuum. Large time steps are allowed while keeping accuracy on smooth solutions even for low Mach number flows.

Keywords. Lagrange-projection; discontinuous Galerkin method; explicit-implicit; entropy-satisfying; positivity-preserving; compressible Euler equations

AMS subject classifications. 65M12; 65M60

1. Introduction

This work pursues the nonlinear analysis of a robust high-order space-time integration method for the description of transport phenomena in fluid flows [22]. In many applications these phenomena are associated to slow waves compared to the fast acoustic waves and require accurate resolution, a classical example being the numerical simulation of low speed flows. Numerical methods are however usually designed for the resolution of all waves and suffer from restriction of the fast waves. In standard explicit shock-capturing methods the time step is limited by the fast waves to ensure stability of the numerical scheme. Moreover, their numerical diffusion is proportional to the speed of the fastest waves and impose over-resolution in space and time.

Our objective here is to describe accurately the transport phenomena, while relaxing the time step constraint due to the acoustic waves via a CFL condition. For that purpose, we consider a Lagrange-projection (LP) like method introduced in [10] in the context of a first-order finite volume discretization of the Euler equations. This method uses the Lagrange-projection framework [15] for the splitting of acoustic and transport operators, but no mesh movement is applied. The acoustic operator is solved in Lagrangian coordinates, while the projection onto the grid is replaced by the transport operator. The Lagrange step is integrated in time with an implicit backward-Euler scheme in order to relax the time step restriction associated to acoustic waves. An explicit forward Euler method is applied to the transport step in order to accurately describe associated unsteady phenomena. A relaxation scheme is then used for the

*Received: July 6, 2016; accepted (in revised form): October 21, 2016. Communicated by Siddhartha Mishira.

†ONERA The French Aerospace Lab, 92320 Châtillon Cedex, France (florent.renac@onera.fr).

approximation of nonlinearities associated to the equation of state [9,13] which consists in using an approximate quasi-linear system with stiff relaxation source terms for the design of an efficient approximate Riemann solver for the Euler equations. This method was then extended to high orders of approximation in [22] by using a discontinuous Galerkin (DG) method [17,18] and constitutes the LPDG scheme. DG discretizations are now widely used for the solution of nonlinear convection dominated flow problems [7,8,14,23–25]. The analysis of this scheme in [22] was restricted to the isentropic Euler equations and established conditions on the time step and on a parameter setting the amount of numerical dissipation to guaranty positivity of density and satisfy a discrete entropy inequality.

We note that the present work share some similarities with preceding contributions from the literature. The high-order DG discretization of a LP like method was first proposed in [11] where the use of a linearized Riemann solver allowed one to prove an entropy inequality for the acoustic step similar to the one in Equation (4.20). The discretization of the convective step was different, however, and no results for positivity and stability were established for the whole LP step. The method was then successfully applied to the multi-dimensional Euler equations in axisymmetric geometry in [12]. Other approaches for the discretization of the Euler equations in Lagrangian coordinates may also be found in [29,30].

On the one hand, the present work addresses two limitations of the LPDG scheme in [22]: the restriction to the isentropic Euler equations and a global parameter tuning the numerical dissipation. First, the numerical scheme is extended to the compressible Euler equations with a general equation of state. We derive conditions to guaranty positivity of the mean values of the discrete density and internal energy, as well as to satisfy a discrete inequality for the physical entropy. Compared to the work in [22], the proof for the entropy inequality uses an argument based on reversing the roles of energy conservation and entropy inequality as initially introduced in [9]. Then, conditions for positivity and stability are given for a numerical dissipation parameter evaluated locally in each mesh element. This aspect is important to keep accuracy in smooth regions of the flow where large numerical dissipation is not needed. The effect of the numerical flux on the quality of the approximation is known to decrease as the polynomial degree p in the DG method increases [8, 20, 21]. However, the present method is based on a relaxation approximation [4,5,9,13] of the Euler equations with a quasi-linear enlarged system thus introducing dissipation through the PDE model. In order to limit this effect, we derive an evolution equation for the Lagrangian sound speed which allows one to evaluate locally the numerical dissipation needed to satisfy a subcharacteristic condition for stability. This strategy is also used for instance to design schemes adapted to vacuum [3].

On the other hand, the scheme is designed with the objective of overcoming issues related to over-resolution in space and time in the low Mach number limit. The acoustic terms are integrated with an implicit time discretization, while the use of characteristic variables in the discrete acoustic scheme avoids the divergence of the numerical dissipation as the Mach number tends to zero. A scale analysis of the truncation error of the discrete scheme in the low Mach number limit as well as numerical experiments support the relevance of this approach.

Finally, the properties of the numerical scheme are satisfied by the mean value of the numerical solution in the elements of the mesh in the same spirit as the positivity preserving scheme in [19] and the entropy satisfying scheme in [1]. *A posteriori* limiters introduced in [31,32] are then applied to extend the properties to nodal values within

elements.

The paper is organized as follows. Section 2 presents the model problem with the system of compressible Euler equations (Section 2.1) and the splitting between acoustic and transport operators together with the relaxation approximation of the acoustic step (Section 2.2). The numerical approach for the high-order space discretization is introduced in Section 3, while time discretization is described in Section 4. The first-order implicit-explicit time integration is described in Section 4.1, the properties of the numerical scheme are analyzed in Section 4.2, low Mach number behavior is investigated in Section 4.3, and limiting strategies are discussed in Section 4.4. These results are assessed by several numerical experiments in Section 5. Finally, concluding remarks about this work are given in Section 6.

2. One-dimensional model problem

2.1. Compressible Euler equations. The discussion in this paper focuses on the compressible Euler equations in one space dimension. Let $\Omega = \mathbb{R}$ be the space domain and consider the following problem

$$\partial_t \mathbf{u} + \partial_x \mathbf{f}(\mathbf{u}) = 0, \qquad \text{in } \Omega \times (0,\infty), \tag{2.1a}$$

$$\mathbf{u}(\cdot,0) = \mathbf{u}_0(\cdot), \quad \text{in } \Omega, \tag{2.1b}$$

where

$$\mathbf{u} = \begin{pmatrix} \rho \\ \rho u \\ \rho E \end{pmatrix}, \quad \mathbf{f}(\mathbf{u}) = \begin{pmatrix} \rho u \\ \rho u^2 + \mathrm{p} \\ (\rho E + \mathrm{p})u \end{pmatrix}$$

represent the conservative variables and nonlinear convective fluxes with ρ the density, u the velocity, $E = e + u^2/2$ the specific total energy, and e the specific internal energy. Equations (2.1) are supplemented with a general equation of state for the specific internal energy of the form $e = e(\tau, \mathrm{s})$ with $\tau = 1/\rho$ the specific volume and s the specific entropy defined by the first and second laws of thermodynamics

$$T d\mathrm{s} = de + \mathrm{p} d\tau,$$

with T the temperature. Under classical assumptions, the pressure may be defined by $\mathrm{p} = -(\partial_\tau e)_\mathrm{s}$ through the relation $\mathrm{p} = \mathrm{p}(\tau, \mathrm{s})$. The system (2.1a) is strictly hyperbolic over the set of states

$$\Omega^a = \{\mathbf{u} \in \mathbb{R}^3 : \rho > 0, u \in \mathbb{R}, E - \tfrac{u^2}{2} > 0\},$$

with eigenvalues $\mu_1 = u - c$, $\mu_3 = u + c$ associated to nonlinear fields and $\mu_2 = u$ associated to a linearly degenerate field. The sound speed is defined by $c(\tau, \mathrm{s}) = \sqrt{-\tau^2 (\partial_\tau \mathrm{p})_\mathrm{s}}$.

Note that it will be useful in the following to also express the internal energy and entropy as functions of the conservative variables: $e(\mathbf{u}) = \big(\rho E - (\rho u)^2/2\rho\big)/\rho$ and $\mathrm{s}(\mathbf{u}) = \mathrm{s}\big(1/\rho, e(\mathbf{u})\big)$.

It may be easily verified that the mapping $\mathcal{U} : \Omega^a \ni \mathbf{u} \mapsto \mathcal{U}(\mathbf{u}) = -\rho \mathrm{s}(\mathbf{u}) \in \mathbb{R}$ is a strictly convex function [15]. Physically relevant solutions to the problem (2.1) must hence satisfy an inequality of the form

$$\partial_t \mathcal{U} + \partial_x (\mathcal{U} u) \leq 0. \tag{2.2}$$

2.2. Acoustic-transport operator splitting. Following [10,22], we decompose the system (2.1a) between acoustic and transport operators with a sequential splitting: the acoustic step reads

$$\partial_t \mathbf{u} + (\partial_x u)\mathbf{u} + \partial_x \begin{pmatrix} 0 \\ \mathrm{p} \\ \mathrm{p}u \end{pmatrix} = 0; \tag{2.3}$$

then, setting $\mathbf{f}_t(\mathbf{u}) = u\mathbf{u}$, the transport step reads

$$\partial_t \mathbf{u} + \partial_x \mathbf{f}_t(\mathbf{u}) - (\partial_x u)\mathbf{u} = 0. \tag{2.4}$$

Let m be the mass variable defined by $dm = \rho_0(x)dx$. We approximate the space derivative operator $\tau\partial_x$ by $\tau(x,0)\partial_x$ with $\tau(\cdot,0) = 1/\rho_0(\cdot)$ in the acoustic step. Assuming smooth solutions, the system (2.3) may be rewritten into the equivalent form

$$\partial_t \tau - \partial_m u = 0, \quad \partial_t u + \partial_m \mathrm{p} = 0, \quad \partial_t E + \partial_m(\mathrm{p}u) = 0. \tag{2.5}$$

Solutions to the acoustic step (2.5) may be approximated by solutions of the following Suliciu relaxation system [5]

$$\partial_t \mathbf{w} + \partial_m \mathbf{f}_a(\mathbf{w}) = \mathbf{s}(\mathbf{w}), \tag{2.6}$$

with

$$\mathbf{w} = \begin{pmatrix} \tau \\ u \\ E \\ \frac{\Pi}{a^2} \\ a \end{pmatrix}, \quad \mathbf{f}_a(\mathbf{w}) = \begin{pmatrix} -u \\ \Pi \\ \Pi u \\ u \\ 0 \end{pmatrix}, \quad \mathbf{s}(\mathbf{w}) = \begin{pmatrix} 0 \\ 0 \\ 0 \\ -\frac{\Pi - \mathrm{p}(\tau,\mathrm{s})}{a^2\varepsilon} \\ 0 \end{pmatrix}, \tag{2.7}$$

where $\varepsilon > 0$ represents a characteristic relaxation time. Equation (2.6d) models the evolution of the pressure relaxation, Π, in flows subject to mechanical disequilibrium. The variable Π may be viewed as a linearization of the pressure p around its *equilibrium*, $\Pi = \mathrm{p}(\tau,\mathrm{s})$, while $a > 0$ is a parameter that approximates the Lagrangian sound speed, ρc. It may be shown that the relaxation system (2.6) is a dissipative approximation of the acoustic step (2.5) under the subcharacteristic condition

$$a > \max_{\tau,\mathrm{s}} \sqrt{-\left(\frac{\partial \mathrm{p}}{\partial \tau}\right)_{\mathrm{s}}}, \tag{2.8}$$

for all τ and s under consideration. In the limit of instantaneous relaxation this ensures that

$$\lim_{\varepsilon \to 0} \Pi = \mathrm{p}(\tau,\mathrm{s}), \tag{2.9}$$

and system (2.6) converges formally toward the system (2.5). We refer the reader to [5,9] for an in-depth discussion on the relaxation approximation of the Euler equations.

With a slight abuse, in the following the whole vector $\mathbf{w}$ will be referred to as the Lagrange variables. We note that the choice of the non uniform relaxation parameter, a, in the system (2.6) will allow to locally adapt the amount of numerical dissipation of the numerical scheme (see Section 4.1).

It may be shown that the homogeneous system (2.6) is hyperbolic over the set of states

$$\Omega^r = \{\mathbf{w}\in\mathbb{R}^5 : \rho>0, u\in\mathbb{R}, E-\tfrac{u^2}{2}>0, \Pi\in\mathbb{R}, a>0\},$$

with eigenvalues $\mu_1=-a<\mu_2=\mu_3=\mu_4=0<\mu_5=a$ associated to linearly degenerate fields. The characteristic variables associated with these eigenvalues are $\overleftarrow{w}=\Pi-au$, $J=\Pi+a^2\tau$, $Y=e-\Pi^2/2a^2$, a, and $\overrightarrow{w}=\Pi+au$, respectively, and satisfy

$$\partial_t \overleftarrow{w} - a(\partial_m\Pi - a\partial_m u) = 0, \tag{2.10a}$$
$$\partial_t J = 0, \tag{2.10b}$$
$$\partial_t Y = 0, \tag{2.10c}$$
$$\partial_t a = 0, \tag{2.10d}$$
$$\partial_t \overrightarrow{w} + a(\partial_m\Pi + a\partial_m u) = 0. \tag{2.10e}$$

Moreover, one may easily solve the Riemann problem defined by system (2.6) without source terms, i.e., $\varepsilon\to\infty$, associated with the initial condition $\mathbf{w}(m,0)=\mathbf{w}_L$ if $m<0$ or $\mathbf{w}(m,0)=\mathbf{w}_R$ if $m>0$, where $\mathbf{w}_L$ and $\mathbf{w}_R$ are in Ω^r. The unique solution to this problem is the self-similar solution $\boldsymbol{\mathcal{W}}(\cdot;\mathbf{w}_L,\mathbf{w}_R)$ defined by

$$\boldsymbol{\mathcal{W}}(\tfrac{m}{t};\mathbf{w}_L,\mathbf{w}_R) = \begin{cases} \mathbf{w}_L, & \frac{m}{t}<-a_L,\\ \mathbf{w}_L^\star, & -a_L<\frac{m}{t}<0,\\ \mathbf{w}_R^\star, & 0<\frac{m}{t}<a_R,\\ \mathbf{w}_R, & \frac{m}{t}>a_R, \end{cases} \tag{2.11}$$

where $\mathbf{w}_L^\star=(\tau_L^\star,u^\star,E_L^\star,\Pi^\star/a_L^2,a_L)^\top$, $\mathbf{w}_R^\star=(\tau_R^\star,u^\star,E_R^\star,\Pi^\star/a_R^2,a_R)^\top$, and

$$u^\star = \tfrac{a_Lu_L+a_Ru_R+\Pi_L-\Pi_R}{a_L+a_R}, \tag{2.12a}$$
$$\Pi^\star = \tfrac{a_R\Pi_L+a_L\Pi_R+a_La_R(u_L-u_R)}{a_L+a_R}, \tag{2.12b}$$
$$\tau_L^\star = \tau_L+\tfrac{u^\star-u_L}{a_L}, \quad \tau_R^\star = \tau_R+\tfrac{u_R-u^\star}{a_R}, \tag{2.12c}$$
$$E_L^\star = E_L-\tfrac{\Pi^\star u^\star-\Pi_Lu_L}{a_L}, \quad E_R^\star = E_R-\tfrac{\Pi_Ru_R-\Pi^\star u^\star}{a_R}. \tag{2.12d}$$

Indeed, using the linear degeneracy of fields associated to eigenvalues $\mu_1=-a$ and $\mu_5=a$, we obtain $a_L^\star=a_L$ and $a_R^\star=a_R$. The Rankine–Hugoniot relations associated with the continuity and momentum Equations (2.6a,b) through the steady 2-wave impose $u_L^\star=u_R^\star=u^\star$ and $\Pi_L^\star=\Pi_R^\star=\Pi^\star$. Now, applying the Rankine–Hugoniot relations across the 1- and 5-waves, one obtains

$$-a_L(\tau_L^\star-\tau_L)+(u^\star-u_L)=0, \tag{2.13a}$$
$$a_R(\tau_R-\tau_R^\star)+(u_R-u^\star)=0, \tag{2.13b}$$
$$-a_L(u^\star-u_L)-(\Pi^\star-\Pi_L)=0, \tag{2.13c}$$
$$a_R(u_R-u^\star)-(\Pi_R-\Pi^\star)=0, \tag{2.13d}$$
$$-a_L(E_L^\star-E_L)-(\Pi^\star u^\star-\Pi_Lu_L)=0, \tag{2.13e}$$
$$a_R(E_R-E_R^\star)-(\Pi_Ru_R-\Pi^\star u^\star)=0. \tag{2.13f}$$

Adding and subtracting Equations (2.13c) and (2.13d), one obtains the expressions for $u^\star$ and $\Pi^\star$, respectively. Then, Equations (2.13a) and (2.13b) lead to the expressions (2.12c), while Equations (2.13e) and (2.13f) give Equation (2.12d).

3. Discontinuous Galerkin formulation

The DG method consists in defining a discrete weak formulation of problem (2.4), (2.6), and (2.1b). The domain is discretized with a grid $\Omega_h = \cup_{j\in\mathbb{Z}}\kappa_j$ with cells $\kappa_j = [x_{j-\frac{1}{2}}, x_{j+\frac{1}{2}}]$, $x_{j+\frac{1}{2}} = (j+\frac{1}{2})h$ and $h>0$ the space step (see Figure 3.1) that we assume to be uniform without loss of generality.

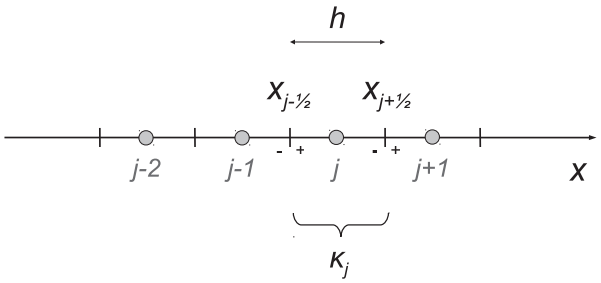

FIG. 3.1. *Mesh with definition of left and right traces at interfaces* $x_{j\pm\frac{1}{2}}$.

3.1. Numerical solution. We look for approximate solutions in the function space of discontinuous polynomials $\mathcal{V}_h^p = \{v_h \in L^2(\Omega_h) : v_h|_{\kappa_j} \in \mathcal{P}_p(\kappa_j), \kappa_j \in \Omega_h\}$, where $\mathcal{P}_p(\kappa_j)$ denotes the space of polynomials of degree at most p in the element κ_j. The approximate solution to the Euler Equations (2.1) is sought under the form

$$\mathbf{u}_h(x,t) = \sum_{l=0}^{p} \phi_j^l(x)\mathbf{U}_j^l(t), \quad \forall x\in\kappa_j, \kappa_j\in\Omega_h, t\geq 0, \tag{3.1}$$

where $\mathbf{U}_j^l = (\rho_j^l, \rho U_j^l, \rho E_j^l)^\top$ constitute the degrees of freedom (DOFs) in the element κ_j and are associated to conservative variables. The subset $(\phi_j^0,\dots,\phi_j^p)$ constitutes a basis of $\mathcal{V}_h^p$ restricted onto a given element. In this work we will use the Lagrange interpolation polynomials $\ell_{0\leq k\leq p}$ associated to the Gauss–Lobatto nodes over the segment $[-1,1]$: $s_0 = -1 < s_1 < \cdots < s_p = 1$:

$$\ell_k(s_l) = \delta_{k,l}, \quad 0\leq k,l\leq p, \tag{3.2}$$

with $\delta_{k,l}$ the Kronecker symbol. The basis functions in a given element κ_j thus read $\phi_j^k(x) = \ell_k(\sigma_j(x))$, where $\sigma_j(x) = 2(x-x_j)/h$ and $x_j = (x_{j+\frac{1}{2}} + x_{j-\frac{1}{2}})/2$ denotes the center of the element.

The DOFs thus correspond to the point values of the solution, e.g., given $0\leq k\leq p$, j in $\mathbb{Z}$, and $t\geq 0$, we have $\mathbf{u}_h(x_j^k,t) = \mathbf{U}_j^k(t)$ for $x_j^k = x_j + s_k h/2$. The left and right traces of the numerical solution at interfaces $x_{j\pm\frac{1}{2}}$ of a given element hence read (see Figure 3.1):

$$\mathbf{u}_{j+\frac{1}{2}}^-(t) := \mathbf{u}_h(x_{j+\frac{1}{2}}^-,t) = \mathbf{U}_j^p(t), \quad \forall t\geq 0, \tag{3.3a}$$

$$\mathbf{u}_{j-\frac{1}{2}}^+(t) := \mathbf{u}_h(x_{j-\frac{1}{2}}^+,t) = \mathbf{U}_j^0(t), \quad \forall t\geq 0. \tag{3.3b}$$

For the discretization of Equations (2.6), we use the interpolation polynomials

$$\mathbf{w}_h(x,t) = \sum_{l=0}^{p} \phi_j^l(x)\mathbf{W}_j^l(t), \quad \forall x\in\kappa_j, \kappa_j\in\Omega_h, t\geq 0, \tag{3.4}$$

where $\mathbf{W}_j^l = (\tau_j^l, U_j^l, E_j^l, \Pi_j^l/a_j^2, a_j)^\top$ are coefficients associated to Lagrange variables. Note that a_j is now a numerical parameter and is assumed to be uniform within each element κ_j. In the following, we will also use nodal values of entropy and internal energy:

$$S_j^l(t) = \mathrm{s}\big(\tau_j^l(t), e_j^l(t)\big), \quad e_j^l(t) = E_j^l(t) - \frac{(U_j^l(t))^2}{2}. \tag{3.5}$$

Moreover, assuming equilibrium $\varepsilon \to 0$ for the relaxation system (2.6), the physical and relaxation pressures satisfy

$$\Pi_j^k(t) = \mathrm{p}\big(\tau_j^k(t), S_j^k(t)\big), \quad 0 \le k \le p, \quad t > 0. \tag{3.6}$$

As a consequence, the conservative (3.1) and Lagrange variables (3.4) may be related in a weak sense by the relations

$$\mathbf{W}_j^k(t) = \mathbf{w}(\mathbf{U}_j^k(t)) \quad 0 \le k \le p, \quad t \ge 0, \tag{3.7a}$$

$$\mathbf{U}_j^k(t) = \mathbf{u}(\mathbf{W}_j^k(t)) \quad 0 \le k \le p, \quad t \ge 0, \tag{3.7b}$$

where

$$\mathbf{w} : \Omega^a \to \Omega^r \ ; \ \mathbf{u} \mapsto \mathbf{w}(\mathbf{u}) = \Big(\tfrac{1}{\rho}, \tfrac{\rho u}{\rho}, \tfrac{\rho E}{\rho}, \tfrac{1}{a^2}\mathrm{p}\big(\tfrac{1}{\rho}, \mathrm{s}\big(\tfrac{1}{\rho}, \tfrac{\rho E}{\rho} - \tfrac{(\rho u)^2}{2\rho^2}\big)\big), a\Big)^\top,$$

$$\mathbf{u} : \Omega^r \to \Omega^a \ ; \ \mathbf{w} \mapsto \mathbf{u}(\mathbf{w}) = \Big(\tfrac{1}{\tau}, \tfrac{u}{\tau}, \tfrac{E}{\tau}\Big)^\top,$$

denote, with a slight abuse, the change from conservative to Lagrange variables and its inverse, a being evaluated from the condition (2.8).

3.2. Space discretization. We follow the method introduced in [22] for the space discretization. Substitute Equation (3.4) into the acoustic step without source term, i.e., the system (2.6) with $\varepsilon \to \infty$. Multiply it with a test function v_h in $\mathcal{V}_h^p$ with support in a given element κ_j and integrate by parts over κ_j to obtain

$$\int_{\kappa_j} v_h \partial_t \mathbf{w}_h dx - \int_{\kappa_j} \mathbf{f}_a(\mathbf{w}_h) \partial_x(v_h \tau_h) dx + \Big[v_h \tau_h \mathbf{h}_a(\mathbf{w}_h^-, \mathbf{w}_h^+)\Big]_{x_{j-\frac{1}{2}}}^{x_{j+\frac{1}{2}}} = 0,$$

where the physical flux at interfaces has been replaced by the numerical flux defined from the solution of the Riemann problem (2.11):

$$\mathbf{h}_a(\mathbf{w}_{j+\frac{1}{2}}^-, \mathbf{w}_{j+\frac{1}{2}}^+) = \mathbf{f}_a\big(\boldsymbol{\mathcal{W}}(0; \mathbf{w}_{j+\frac{1}{2}}^-, \mathbf{w}_{j+\frac{1}{2}}^+)\big) = \begin{pmatrix} -u_{j+\frac{1}{2}}^\star \\ \Pi_{j+\frac{1}{2}}^\star \\ \Pi_{j+\frac{1}{2}}^\star u_{j+\frac{1}{2}}^\star \\ u_{j+\frac{1}{2}}^\star \\ 0 \end{pmatrix}, \tag{3.8}$$

with data at equilibrium, i.e., $\Pi_{j+\frac{1}{2}}^\pm = \mathrm{p}\big(\tau_{j+\frac{1}{2}}^\pm, \mathrm{s}(\tau_{j+\frac{1}{2}}^\pm, e_{j+\frac{1}{2}}^\pm)\big)$.

Using a second integration by parts of the second integral, the semi-discrete equation may be equivalently written as

$$\int_{\kappa_j} v_h \partial_t \mathbf{w}_h dx + \int_{\kappa_j} v_h \tau_h \partial_x \mathbf{f}_a(\mathbf{w}_h) dx + \Big[v_h \tau_h \big(\mathbf{h}_a(\mathbf{w}_h^-, \mathbf{w}_h^+) - \mathbf{f}_a(\mathbf{w}_h)\big)\Big]_{x_{j-\frac{1}{2}}}^{x_{j+\frac{1}{2}}} = 0. \tag{3.9}$$

Likewise, considering the approximate solution (3.1) for the space discretization of the transport problem (2.4), the semidiscrete form reads

$$\int_{\kappa_j} v_h \partial_t \mathbf{u}_h dx + \int_{\kappa_j} (v_h u_h) \partial_x \mathbf{u}_h dx + \Big[v_h \big(\mathbf{h}_t(\mathbf{u}_h^-, \mathbf{u}_h^+) - h_u(u_h^-, u_h^+) \mathbf{u}_h \big) \Big]_{x_{j-\frac{1}{2}}}^{x_{j+\frac{1}{2}}} = 0, \quad (3.10)$$

where $\mathbf{h}_t : \Omega^a \times \Omega^a \to \mathbb{R}^3$ and $h_u : \mathbb{R} \times \mathbb{R} \to \mathbb{R}$ denote upwind numerical fluxes consistent with the physical fluxes of the transport step: $\mathbf{h}_t(\mathbf{u}, \mathbf{u}) = u\mathbf{u}$ and $h_u(u, u) = u$. Introducing

$$\hat{\mathbf{u}}_{j+\frac{1}{2}} = \begin{cases} \mathbf{U}_j^p, & u_{j+\frac{1}{2}}^\star > 0, \\ \mathbf{U}_{j+1}^0, & u_{j+\frac{1}{2}}^\star \leq 0, \end{cases} \quad (3.11)$$

where the quantity $u_{j+\frac{1}{2}}^\star$ is defined from the numerical flux (3.8) for the acoustic step, we set

$$\mathbf{h}_t(\mathbf{u}_{j+\frac{1}{2}}^-, \mathbf{u}_{j+\frac{1}{2}}^+) = u_{j+\frac{1}{2}}^\star \hat{\mathbf{u}}_{j+\frac{1}{2}} = (u_{j+\frac{1}{2}}^\star)^+ \mathbf{U}_j^p + (u_{j+\frac{1}{2}}^\star)^- \mathbf{U}_{j+1}^0, \quad (3.12)$$

where

$$(u_{j+\frac{1}{2}}^\star)^+ = \max(u_{j+\frac{1}{2}}^\star, 0), \quad (u_{j+\frac{1}{2}}^\star)^- = \min(u_{j+\frac{1}{2}}^\star, 0),$$

represent positive and negative parts of $u_{j+\frac{1}{2}}^\star$. Then, we set

$$h_u(u_{j+\frac{1}{2}}^-, u_{j+\frac{1}{2}}^+) = u_{j+\frac{1}{2}}^\star. \quad (3.13)$$

Following [22], the integrals in the semidiscrete Equations (3.9) and (3.10) are approximated by using a Gauss–Lobatto quadrature with nodes collocated with the interpolation points of the numerical solution

$$\int_{\kappa_j} f(x) dx \simeq \frac{h}{2} \sum_{l=0}^{p} \omega_l f(x_j^l),$$

with $\omega_l > 0$, $\sum_{l=0}^p \omega_l = 2$, $x_j^l = x_j + s_l h/2$ the weights and nodes of the quadrature rule, and s_l defined in Equation (3.2). This leads to the definition of the discrete inner product in the element κ_j

$$\langle f, g \rangle_j^p = \frac{h}{2} \sum_{l=0}^{p} \omega_l f(x_j^l) g(x_j^l).$$

The integration by parts used in Equations (3.9) and (3.10) are thus replaced by summation by parts. As noticed in [16], this operation holds true in a weak sense for general functions f by considering its interpolation polynomial of degree p at integration points: $f_h(\cdot) = \sum_{l=0}^p f(x_j^l) \phi_j^l(\cdot)$.

The present collocation strategy is important for the theoretical analysis in Section 4 as it allows simple evaluation of integrals and trace values of the solution at interfaces.

4. Time discretization

4.1. First-order time discretization. Let $t^{(n)}=n\Delta t$, with $\Delta t>0$ the time step, and use the notation $\mathbf{u}_h^{(n)}(\cdot)=\mathbf{u}_h(\cdot,t^{(n)})$. The time integration of the Euler equations with LP over a time step is done with a sequential splitting: homogeneous acoustic step (3.9) over $(t^{(n)},t^{(n+1^-)}]$ and transport step (3.10) over $(t^{(n+1^-)},t^{(n+1)}]$. Relaxation mechanisms in the system (2.6) are taken into account by imposing data at equilibrium at each time step: $\Pi_j^k(t^{(n)})=\mathrm{p}\big(\tau_j^k(t^{(n)}),S_j^k(t^{(n)})\big)$ with $S_j^k(t^{(n)})$ defined by Equations (3.5).

We use an implicit backward-Euler scheme for the time discretization of the acoustic step over $(t^{(n)},t^{(n+1^-)}]$. Approximating the mass variable by $\Delta m=\tau_j^k(t^{(n)})h$ at point x_j^k over $(t^{(n)},t^{(n+1^-)}]$ and setting $v_h=\phi_j^k$ into (3.9), the discrete scheme now reads

$$\begin{aligned}\mathbf{W}_j^{k,n+1^-}=\mathbf{W}_j^{k,n}-\lambda_k\tau_j^{k,n}\Big[&\big\langle\partial_x\mathbf{f}_a(\mathbf{w}_h^{n+1^-}),\phi_j^k\big\rangle_j^p\\&+\delta_{k,p}\big(\mathbf{h}_a(\mathbf{W}_j^{p,n+1^-},\mathbf{W}_{j+1}^{0,n+1^-})-\mathbf{f}_a(\mathbf{W}_j^{p,n+1^-})\big)\\&-\delta_{k,0}\big(\mathbf{h}_a(\mathbf{W}_{j-1}^{p,n+1^-},\mathbf{W}_j^{0,n+1^-})-\mathbf{f}_a(\mathbf{W}_j^{0,n+1^-})\big)\Big],\end{aligned}\tag{4.1}$$

for all $0\le k\le p$ and j in $\mathbb{Z}$, where we have used the notations $\mathbf{W}_j^{k,n}=\mathbf{W}_j^k(t^{(n)})$ and $\lambda_k=2\lambda/\omega_k$ with $\lambda=\Delta t/h$. without any possible confusion on the time and trace values.

The last equation in the system (4.1) imposes $a_j^{n+1^-}=a_j^n$, so a_j is constant over the whole time step $(t^{(n)},t^{(n+1)}]$. The subcharacteristic condition (2.8) is then imposed at the discrete level by requiring that

$$a_j^n>\max_{0\le k\le p}\max_{\theta\in[0,1]}\sqrt{-\partial_\tau\mathrm{p}\big(\theta\tau_j^{k,n}+(1-\theta)\tau_j^{k,n+1^-},S_j^{k,n}\big)},\quad n\in\mathbb{N},\quad j\in\mathbb{Z}.\tag{4.2}$$

Likewise, we use an explicit forward Euler time integration of the semidiscrete transport Equations (3.10). Introducing the definitions of the numerical fluxes (3.12) and (3.13), we obtain

$$\begin{aligned}\mathbf{U}_j^{k,n+1}=\mathbf{U}_j^{k,n+1^-}-\lambda_k\Big[&\big\langle u_h^{n+1^-}\partial_x\mathbf{u}_h^{n+1^-},\phi_j^k\big\rangle_j^p\\&+\delta_{k,p}u_{j+\frac12}^{\star,n+1^-}\big(\hat{\mathbf{u}}_{j+\frac12}^{n+1^-}-\mathbf{U}_j^{p,n+1^-}\big)-\delta_{k,0}u_{j-\frac12}^{\star,n+1^-}\big(\hat{\mathbf{u}}_{j-\frac12}^{n+1^-}-\mathbf{U}_j^{0,n+1^-}\big)\Big].\end{aligned}\tag{4.3}$$

The discrete problem for the Euler equations now reads: for all times $t^{(n+1)}$ with $n\ge0$ find $\mathbf{u}_h(\cdot,t^{(n+1)})$ in $(\mathcal{V}_h^p)^3$ such that Equations (4.1)–(4.3) are satisfied with

$$\mathbf{W}_j^{k,n}=\mathbf{w}\big(\mathbf{U}_j^{k,n}\big),\quad 0\le k\le p,\quad j\in\mathbb{Z},\tag{4.4a}$$

$$\mathbf{U}_j^{k,n+1^-}=\mathbf{u}\big(\mathbf{W}_j^{k,n+1^-}\big),\quad 0\le k\le p,\quad j\in\mathbb{Z},\tag{4.4b}$$

given by the transformations (3.7).

The time sequence $\mathbf{u}_h(\cdot,t^{(n)})$ is associated with the initial condition $\mathbf{w}_h(\cdot,0)=\mathbf{w}\big(\mathbf{u}_0(\cdot)\big)$ in a weak sense, which reduces to $\mathbf{W}_j^{k,0}=\mathbf{w}\big(\mathbf{u}_0(x_j^k)\big)$ for all $0\le k\le p$ and j in $\mathbb{Z}$.

Note that the acoustic step (4.1) may be rewritten as an implicit problem for the conservative variables. Indeed, we observe that the first component of the discrete Equation (4.1) reads $\tau_j^{k,n+1^-}=L_j^{k,n+1^-}\tau_j^{k,n}$ with

$$L_j^{k,n+1^-}=1+\lambda_k\Big[\big\langle\partial_x u_h^{n+1^-},\phi_j^k\big\rangle_j^p$$

$$+\delta_{k,p}(u_{j+\frac{1}{2}}^{\star,n+1^-}-U_j^{p,n+1^-})-\delta_{k,0}(u_{j-\frac{1}{2}}^{\star,n+1^-}-U_j^{0,n+1^-})\Big]$$
$$=1+\lambda_k\Big[-\big\langle u_h^{n+1^-},d_x\phi_j^k\big\rangle_j^p+\delta_{k,p}u_{j+\frac{1}{2}}^{\star,n+1^-}-\delta_{k,0}u_{j-\frac{1}{2}}^{\star,n+1^-}\Big]. \tag{4.5}$$

Assuming that $\tau_j^{k,n}>0$ and $\tau_j^{k,n+1^-}>0$ (see (4.15) in Lemma 4.1), the first component of the system (4.1) may thus be rewritten under the form

$$L_j^{k,n+1^-}\rho_j^{k,n+1^-}=\rho_j^{k,n}. \tag{4.6}$$

Then, dividing the three first components of the system (4.1) by $\tau_j^{k,n}>0$, using $U_j^{k,n}/\tau_j^{k,n}=L_j^{k,n+1^-}\rho U_j^{k,n+1^-}$ and $E_j^{k,n}/\tau_j^{k,n}=L_j^{k,n+1^-}\rho E_j^{k,n+1^-}$ from Equation (4.6), summing with Equation (4.3) and following the lines in Theorem 3 in [22], one obtains the LPDG scheme which constitutes a conservative approximation consistent in time and space with the Euler Equations (2.1a):

$$\mathbf{U}_j^{k,n+1}=\mathbf{U}_j^{k,n}-\lambda_k\Big[-\big\langle\mathbf{f}(\mathbf{u}_h^{n+1^-}),d_x\phi_j^k\big\rangle_j^p+\delta_{k,p}\mathbf{h}_{j+\frac{1}{2}}^{n+1^-}-\delta_{k,0}\mathbf{h}_{j-\frac{1}{2}}^{n+1^-}\Big], \tag{4.7}$$

with the following numerical flux evaluated from DOFs at time $t^{(n+1^-)}$:

$$\mathbf{h}_{j+\frac{1}{2}}^{n+1^-}=\begin{pmatrix}u_{j+\frac{1}{2}}^{\star,n+1^-}\hat{\rho}_{j+\frac{1}{2}}^{n+1^-}\\ u_{j+\frac{1}{2}}^{\star,n+1^-}\widehat{\rho u}_{j+\frac{1}{2}}^{n+1^-}+\Pi_{j+\frac{1}{2}}^{\star,n+1^-}\\ u_{j+\frac{1}{2}}^{\star,n+1^-}\big(\widehat{\rho E}_{j+\frac{1}{2}}^{n+1^-}+\Pi_{j+\frac{1}{2}}^{\star,n+1^-}\big)\end{pmatrix}. \tag{4.8}$$

Then, we use the numerical scheme (4.1) to establish the discrete versions of the conservation Equations (2.10) for the characteristic variables. First, we set

$$\overrightarrow{W}_j^{k,n}=\Pi_j^{k,n}+a_j^nU_j^{k,n},\quad \overleftarrow{W}_j^{k,n}=\Pi_j^{k,n}-a_j^nU_j^{k,n}. \tag{4.9}$$

We note that from the definition of the numerical flux (3.8) with Equations (2.12), we have

$$\Pi_{j+\frac{1}{2}}^{\star,n+1^-}=\frac{a_{j+1}^n\overrightarrow{W}_j^{p,n+1^-}+a_j^n\overleftarrow{W}_{j+1}^{0,n+1^-}}{a_j^n+a_{j+1}^n},\ u_{j+\frac{1}{2}}^{\star,n+1^-}=\frac{\overrightarrow{W}_j^{p,n+1^-}-\overleftarrow{W}_{j+1}^{0,n+1^-}}{a_j^n+a_{j+1}^n}, \tag{4.10}$$

and we deduce the relations

$$\Pi_{j+\frac{1}{2}}^{\star,n+1^-}+a_j^nu_{j+\frac{1}{2}}^{\star,n+1^-}=\overrightarrow{W}_j^{p,n+1^-},$$
$$\Pi_{j+\frac{1}{2}}^{\star,n+1^-}-a_j^nu_{j+\frac{1}{2}}^{\star,n+1^-}=\frac{(a_{j+1}^n-a_j^n)\overrightarrow{W}_j^{p,n+1^-}+2a_j^n\overleftarrow{W}_{j+1}^{0,n+1^-}}{a_j^n+a_{j+1}^n},$$
$$\Pi_{j-\frac{1}{2}}^{\star,n+1^-}+a_j^nu_{j-\frac{1}{2}}^{\star,n+1^-}=\frac{2a_j^n\overrightarrow{W}_{j-1}^{p,n+1^-}+(a_{j-1}^n-a_j^n)\overleftarrow{W}_j^{0,n+1^-}}{a_{j-1}^n+a_j^n},$$
$$\Pi_{j-\frac{1}{2}}^{\star,n+1^-}-a_j^nu_{j-\frac{1}{2}}^{\star,n+1^-}=\overleftarrow{W}_j^{0,n+1^-}.$$

Using the above relations, simple combinations of equations in the system (4.1) give

$$\overrightarrow{W}_j^{k,n+1^-}=\overrightarrow{W}_j^{k,n}-a_j^n\lambda_k\tau_j^{k,n}\Big[\big\langle\partial_x\overrightarrow{w}_h^{n+1^-},\phi_j^k\big\rangle_j^p$$

$$-\delta_{k,0}\Big(\frac{2a_j^n \overrightarrow{W}_{j-1}^{p,n+1^-} + (a_{j-1}^n - a_j^n)\overleftarrow{W}_j^{0,n+1^-}}{a_{j-1}^n + a_j^n} - \overrightarrow{W}_j^{0,n+1^-}\Big)\Big], \tag{4.11a}$$

$$\tau_j^{k,n+1^-} = \tau_j^{k,n} - \frac{\Pi_j^{k,n+1^-} - \Pi_j^{k,n}}{(a_j^n)^2}, \tag{4.11b}$$

$$E_j^{k,n+1^-} = E_j^{k,n} + U_j^{k,n+1^-}(U_j^{k,n+1^-} - U_j^{k,n}) + \frac{\Pi_j^{k,n+1^-}(\Pi_j^{k,n+1^-} - \Pi_j^{k,n})}{(a_j^n)^2}$$
$$+\frac{\lambda_k \tau_j^{k,n}}{4a_j^n}\Big[\delta_{k,p}\big(\overleftarrow{W}_j^{p,n+1^-} - \overleftarrow{W}_{j+1}^{0,n+1^-}\big)^2 + \delta_{k,0}\big(\overrightarrow{W}_j^{0,n+1^-} - \overrightarrow{W}_{j-1}^{p,n+1^-}\big)^2\Big], \tag{4.11c}$$

$$\overleftarrow{W}_j^{k,n+1^-} = \overleftarrow{W}_j^{k,n} + a_j^n \lambda_k \tau_j^{k,n}\Big[\big\langle \partial_x \overleftarrow{w}_h^{n+1^-}, \phi_j^k \big\rangle_j^p$$
$$+\delta_{k,p}\Big(\frac{(a_{j+1}^n - a_j^n)\overrightarrow{W}_j^{p,n+1^-} + 2a_j^n \overleftarrow{W}_{j+1}^{0,n+1^-}}{a_j^n + a_{j+1}^n} - \overleftarrow{W}_j^{p,n+1^-}\Big)\Big]. \tag{4.11d}$$

The state $\mathbf{u}_h^{n+1^-}$ in the discrete residuals of the LPDG scheme (4.7) is thus evaluated from the linear implicit system (4.11a,d) that may be easily solved for the discrete characteristic variables (4.9) at time $t^{(n+1^-)}$. Then, we use Equations (4.9) to evaluate $U_j^{k,n+1^-}$ and $\Pi_j^{k,n+1^-}$, while $\tau_j^{k,n+1^-}$ and $E_j^{k,n+1^-}$ are given explicitly by (4.11b,c).

Note that compared to the method introduced in [22] for the isentropic Euler equations, the implicit linear system to be solved has the same size. This result is essential for the performances of the present method.

4.2. Properties of the discrete scheme.

4.2.1. Preliminaries. In this section, we discuss the properties of the LPDG scheme with a first-order time integration and arbitrary space discretization order. The main results are given in Theorem 4.1 and prove positivity of density and internal energy for the mean value of the numerical solution, as well as an entropy inequality. The mean value of the numerical solution in a mesh element reads

$$\overline{\mathbf{u}}_j^n := \frac{1}{h}\int_{\kappa_j} \mathbf{u}_h(x, t^{(n)})dx = \sum_{l=0}^{p} \frac{\omega_l}{2}\mathbf{U}_j^{l,n}. \tag{4.12}$$

The entropy inequality applies to $\mathcal{U}$ in the inequality (2.2) that we introduce at the discrete level via its interpolant

$$\mathcal{U}_h(x, t^{(n)}) = -\sum_{l=0}^{p} \phi_j^l(x)\rho S_j^{l,n}, \quad \forall x \in \kappa_j, n \geq 0, \tag{4.13}$$

with $S_j^{l,n} = S_j^l(t^{(n)})$ defined by Equations (3.5).

Before going into the details, let us recall some preliminary results established in [22] that are directly applicable here. These results are reported in Lemma 4.1 and we refer to [22] for the proof.

LEMMA 4.1. *Assume that* $\rho_{j\in\mathbb{Z}}^{0\leq k\leq p,n} > 0$. *Then under the CFL condition*

$$\lambda \max_{j\in\mathbb{Z}} \max_{0\leq k\leq p} \frac{1}{\omega_k}\Big(\big\langle u_h^{n+1^-}, d_x\phi_j^k\big\rangle_j^p - \delta_{k,p}(u_{j+\frac{1}{2}}^{\star,n+1^-})^- + \delta_{k,0}(u_{j-\frac{1}{2}}^{\star,n+1^-})^+\Big) < \frac{1}{2}, \tag{4.14}$$

we have

$$\rho_j^{k,n+1^-} > 0, \tag{4.15}$$

and

$$\overline{\mathbf{u}}_j^{n+1} = \sum_{k=0}^{p} \left(\frac{\omega_k}{2} - \lambda \Big(\big\langle u_h^{n+1^-}, d_x \phi_j^k \big\rangle_j^p - \delta_{k,p} (u_{j+\frac{1}{2}}^{\star,n+1^-})^- + \delta_{k,0} (u_{j-\frac{1}{2}}^{\star,n+1^-})^+ \Big) \right) \mathbf{U}_j^{k,n+1^-} - \lambda (u_{j+\frac{1}{2}}^{\star,n+1^-})^- \mathbf{U}_{j+1}^{0,n+1^-} + \lambda (u_{j-\frac{1}{2}}^{\star,n+1^-})^+ \mathbf{U}_{j-1}^{p,n+1^-} \tag{4.16}$$

is a convex combination of DOFs at time $t^{(n+1^-)}$.

Now, we prove an entropy inequality for the acoustic step in the following lemma.

LEMMA 4.2. *Assume that* $\rho_{j\in\mathbb{Z}}^{0\le k\le p,n} > 0$, *then the discrete acoustic step satisfies the following discrete entropy inequality*

$$\frac{\eta_j^{k,n+1^-} - \eta_j^{k,n}}{2(a_j^n)^2} - \lambda_k \tau_j^{k,n} \Big[\big\langle \Pi_h^{n+1^-} u_h^{n+1^-}, d_x \phi_j^k \big\rangle_j^p - \delta_{k,p} H_{j+\frac{1}{2}}^{n+1^-} + \delta_{k,0} H_{j-\frac{1}{2}}^{n+1^-} \Big] \le 0, \tag{4.17}$$

with

$$\eta_j^{k,n} = \frac{(\overrightarrow{W}_j^{k,n})^2 + (\overleftarrow{W}_j^{k,n})^2}{2}, \quad H_{j+\frac{1}{2}}^{n+1^-} = \Pi_{j+\frac{1}{2}}^{\star,n+1^-} u_{j+\frac{1}{2}}^{\star,n+1^-}, \tag{4.18}$$

and where $\eta_j^{k,n} = \eta\big(\mathbf{w}_h(x_j^k, t^{(n)})\big)$, *with* $0 \le k \le p$, *correspond to the point values in cell* κ_j *of the entropy for the acoustic step (2.6) with* $\eta(\mathbf{w}) = (\overrightarrow{w}^2 + \overleftarrow{w}^2)/2$.

Proof. Multiplying Equation (4.11a) with $\overrightarrow{W}_j^{k,n+1^-}$ gives

$$\begin{aligned} &\frac{(\overrightarrow{W}_j^{k,n+1^-})^2}{2} - \frac{(\overrightarrow{W}_j^{k,n})^2}{2} + a_j^n \lambda_k \tau_j^{k,n} \Big[\overrightarrow{W}_j^{k,n+1^-} \big\langle \partial_x \overrightarrow{w}_h^{n+1^-}, \phi_j^k \big\rangle_j^p \\ &\quad - \delta_{k,0} \overrightarrow{W}_j^{0,n+1^-} \Big(\frac{2a_j^n \overrightarrow{W}_{j-1}^{p,n+1^-} + (a_{j-1}^n - a_j^n) \overleftarrow{W}_j^{0,n+1^-}}{a_{j-1}^n + a_j^n} - \overrightarrow{W}_j^{0,n+1^-} \Big) \Big] \\ &= -\frac{(\overrightarrow{W}_j^{k,n+1^-} - \overrightarrow{W}_j^{k,n})^2}{2}. \end{aligned}$$

Expanding

$$\overrightarrow{W}_j^{k,n+1^-} \big\langle \partial_x \overrightarrow{w}_h^{n+1^-}, \phi_j^k \big\rangle_j^p = \frac{\omega_k h}{2} \overrightarrow{W}_j^{k,n+1^-} \Big(\frac{\partial \overrightarrow{w}_h}{\partial x} \Big)_{x_j^k}^{n+1^-} = \Big\langle \frac{\partial_x (\overrightarrow{w}_h^{n+1^-})^2}{2}, \phi_j^k \Big\rangle_j^p,$$

and using integration by parts, we obtain

$$\begin{aligned} &\frac{(\overrightarrow{W}_j^{k,n+1^-})^2}{2} - \frac{(\overrightarrow{W}_j^{k,n})^2}{2} + a_j^n \lambda_k \tau_j^{k,n} \Big[- \Big\langle \frac{(\overrightarrow{w}_h^{n+1^-})^2}{2}, d_x \phi_j^k \Big\rangle_j^p + \delta_{k,p} \frac{(\overrightarrow{W}_j^{p,n+1^-})^2}{2} \\ &\quad - \delta_{k,0} \Big(\frac{\overrightarrow{W}_j^{0,n+1^-} \big(2a_j^n \overrightarrow{W}_{j-1}^{p,n+1^-} + (a_{j-1}^n - a_j^n) \overleftarrow{W}_j^{0,n+1^-} \big)}{a_{j-1}^n + a_j^n} - \frac{(\overrightarrow{W}_j^{0,n+1^-})^2}{2} \Big) \Big] \le 0. \end{aligned}$$

Likewise, multiplying Equation (4.11d) with $\overleftarrow{W}_j^{k,n+1^-}$ and applying similar manipulations give

$$\frac{(\overleftarrow{W}_j^{k,n+1^-})^2}{2} - \frac{(\overleftarrow{W}_j^{k,n})^2}{2} - a_j^n \lambda_k \tau_j^{k,n} \Big[- \Big\langle \frac{(\overleftarrow{w}_h^{n+1^-})^2}{2}, d_x \phi_j^k \Big\rangle_j^p - \delta_{k,0} \frac{(\overleftarrow{W}_j^{0,n+1^-})^2}{2}$$

$$+\delta_{k,p}\Big(\frac{\overleftarrow{W_j^{p,n+1^-}}\big((a_{j+1}^n-a_j^n)\overrightarrow{W_j^{p,n+1^-}}+2a_j^n\overleftarrow{W_{j+1}^{0,n+1^-}}\big)}{a_j^n+a_{j+1}^n}-\frac{(\overleftarrow{W_j^{p,n+1^-}})^2}{2}\Big)\Big]\leq 0.$$

Summing the two last equations gives

$$\begin{aligned}&\eta_j^{k,n+1^-}-\eta_j^{k,n}+a_j^n\lambda_k\tau_j^{k,n}\Big[-\Big\langle\frac{(\overrightarrow{w_h^{n+1^-}})^2}{2}-\frac{(\overleftarrow{w_h^{n+1^-}})^2}{2},d_x\phi_j^k\Big\rangle_j^p\\&\quad+\delta_{k,p}\Big(\frac{(\overrightarrow{W_j^{p,n+1^-}})^2}{2}+\frac{(\overleftarrow{W_j^{p,n+1^-}})^2}{2}-\frac{\overleftarrow{W_j^{p,n+1^-}}\big((a_{j+1}^n-a_j^n)\overrightarrow{W_j^{p,n+1^-}}+2a_j^n\overleftarrow{W_{j+1}^{0,n+1^-}}\big)}{a_j^n+a_{j+1}^n}\Big)\\&\quad-\delta_{k,0}\Big(\frac{\overrightarrow{W_j^{0,n+1^-}}\big(2a_j^n\overrightarrow{W_{j-1}^{p,n+1^-}}+(a_{j-1}^n-a_j^n)\overleftarrow{W_j^{0,n+1^-}}\big)}{a_{j-1}^n+a_j^n}-\frac{(\overrightarrow{W_j^{0,n+1^-}})^2}{2}-\frac{(\overleftarrow{W_j^{0,n+1^-}})^2}{2}\Big)\Big]\\&\leq 0.\end{aligned}\tag{4.19}$$

Now, the flux contributions in the inequality (4.19) may be transformed in terms of the numerical fluxes in the inequality (4.17). Using (4.10), we get

$$\begin{aligned}\Delta_{j+\frac12}^-&=\frac{(\overrightarrow{W_j^{p,n+1^-}})^2}{2}+\frac{(\overleftarrow{W_j^{p,n+1^-}})^2}{2}-\frac{\overleftarrow{W_j^{p,n+1^-}}\big((a_{j+1}^n-a_j^n)\overrightarrow{W_j^{p,n+1^-}}+2a_j^n\overleftarrow{W_{j+1}^{0,n+1^-}}\big)}{a_j^n+a_{j+1}^n}\\&\quad-2a_j^n\Pi_{j+\frac12}^{\star,n+1^-}u_{j+\frac12}^{\star,n+1^-}\\&=\frac{(\overrightarrow{W_j^{p,n+1^-}})^2}{2}+\frac{(\overleftarrow{W_j^{p,n+1^-}})^2}{2}-\frac{(a_{j+1}^n-a_j^n)\overleftarrow{W_j^{p,n+1^-}}\overrightarrow{W_j^{p,n+1^-}}}{a_j^n+a_{j+1}^n}-\frac{2(a_j^n)^2\overleftarrow{W_j^{p,n+1^-}}\overleftarrow{W_{j+1}^{0,n+1^-}}}{a_j^n+a_{j+1}^n}\\&\quad-\frac{2a_j^na_{j+1}^n(\overleftarrow{W_j^{p,n+1^-}})^2}{a_j^n+a_{j+1}^n}+\frac{2(a_j^n\overleftarrow{W_{j+1}^{0,n+1^-}})^2}{a_j^n+a_{j+1}^n}+\frac{2a_j^n(a_{j+1}^n-a_j^n)\overrightarrow{W_j^{p,n+1^-}}\overleftarrow{W_{j+1}^{0,n+1^-}}}{a_j^n+a_{j+1}^n}\\&=\frac12\Big(\frac{a_{j+1}^n-a_j^n}{a_j^n+a_{j+1}^n}\overrightarrow{W_j^{p,n+1^-}}-\overleftarrow{W_j^{p,n+1^-}}+\frac{2a_j^n}{a_j^n+a_{j+1}^n}\overleftarrow{W_{j+1}^{0,n+1^-}}\Big)^2.\end{aligned}$$

Likewise, we have

$$\begin{aligned}\Delta_{j-\frac12}^+&=\frac{\overrightarrow{W_j^{0,n+1^-}}\big(2a_j^n\overrightarrow{W_{j-1}^{p,n+1^-}}+(a_{j-1}^n-a_j^n)\overleftarrow{W_j^{0,n+1^-}}\big)}{a_{j-1}^n+a_j^n}-\frac{(\overrightarrow{W_j^{0,n+1^-}})^2}{2}-\frac{(\overleftarrow{W_j^{0,n+1^-}})^2}{2}\\&\quad-2a_j^n\Pi_{j-\frac12}^{\star,n+1^-}u_{j-\frac12}^{\star,n+1^-}\\&=-\frac12\Big(\frac{a_j^n-a_{j-1}^n}{a_{j-1}^n+a_j^n}\overleftarrow{W_j^{0,n+1^-}}+\overrightarrow{W_j^{0,n+1^-}}-\frac{2a_j^n}{a_{j-1}^n+a_j^n}\overrightarrow{W_{j-1}^{p,n+1^-}}\Big)^2.\end{aligned}$$

Hence, using $\Delta_{j+\frac12}^-\geq 0$ and $-\Delta_{j-\frac12}^+\geq 0$ in the inequality (4.19) and dividing by $2(a_j^n)^2$ give the inequality (4.17). ∎

4.2.2. Main results. Now let us establish Lemma 4.3 which proves positivity and an entropy inequality for the acoustic step, while Theorem 4.1 states the main results of this work.

LEMMA 4.3. *Assume $\mathbf{U}_{j\in\mathbb{Z}}^{0\leq k\leq p,n}$ are in Ω^a. Then under the CFL condition (4.14) and subcharacteristic condition (4.2), the discrete acoustic step satisfies*

$$e_j^{k,n+1^-}>0,\quad S_j^{k,n+1^-}\geq S_j^{k,n},\tag{4.20}$$

with $S_j^{k,n}$ defined in Equation (4.13) from the point values of the specific entropy.

Proof. We follow the idea introduced in [9] (see also [3], Section 2.4) consisting in reversing the roles of energy conservation and entropy inequality. First consider the following system over the time interval $(t^{(n)},t^{(n+1^{\#})}]\subset(t^{(n)},t^{(n+1^{-})}]$:

$$\partial_t\tau-\partial_m u=0,\quad \partial_t u+\partial_m \mathrm{p}=0,\quad \partial_t \mathrm{s}=0, \tag{4.21}$$

together with the entropy inequality for the strictly convex mapping $(\tau,u,\mathrm{s})\mapsto E(\tau,u,\mathrm{s})$:

$$\partial_t E+\partial_m(\mathrm{p}u)\leq 0.$$

Using the same procedure as the one introduced in Section 3 for the space-time discretization, we obtain the following discrete scheme for the system (4.21):

$$\begin{aligned}
\tau_j^{k,n+1^{\#}} &= \tau_j^{k,n}+\lambda_k\tau_j^{k,n}\Big[\big\langle\partial_x u_h^{n+1^{\#}},\phi_j^k\big\rangle_j^p+\delta_{k,p}\big(u_{j+\frac12}^{\star,n+1^{\#}}-U_j^{p,n+1^{\#}}\big)\\
&\quad -\delta_{k,0}\big(u_{j-\frac12}^{\star,n+1^{\#}}-U_j^{0,n+1^{\#}}\big)\Big], &(4.22a)\\
U_j^{k,n+1^{\#}} &= U_j^{k,n}-\lambda_k\tau_j^{k,n}\Big[\big\langle\partial_x \Pi_h^{n+1^{\#}},\phi_j^k\big\rangle_j^p+\delta_{k,p}\big(\Pi_{j+\frac12}^{\star,n+1^{\#}}-\Pi_j^{p,n+1^{\#}}\big)\\
&\quad -\delta_{k,0}\big(\Pi_{j-\frac12}^{\star,n+1^{\#}}-\Pi_j^{0,n+1^{\#}}\big)\Big], &(4.22b)\\
S_j^{k,n+1^{\#}} &= S_j^{k,n} &(4.22c)\\
\Pi_j^{k,n+1^{\#}} &= \Pi_j^{k,n}-(a_j^n)^2\lambda_k\tau_j^{k,n}\Big[\big\langle\partial_x u_h^{n+1^{\#}},\phi_j^k\big\rangle_j^p+\delta_{k,p}\big(u_{j+\frac12}^{\star,n+1^{\#}}-U_j^{p,n+1^{\#}}\big)\\
&\quad -\delta_{k,0}\big(u_{j-\frac12}^{\star,n+1^{\#}}-U_j^{0,n+1^{\#}}\big)\Big]. &(4.22d)
\end{aligned}$$

Applying Lemma 4.2, the scheme satisfies for the entropy of the acoustic step (2.6) the inequality

$$\tfrac{\eta_j^{k,n+1^{\#}}-\eta_j^{k,n}}{2(a_j^n)^2}-\lambda_k\tau_j^{k,n}\Big[\big\langle\Pi_h^{n+1^{\#}}u_h^{n+1^{\#}},d_x\phi_j^k\big\rangle_j^p-\delta_{k,p}H_{j+\frac12}^{n+1^{\#}}+\delta_{k,0}H_{j-\frac12}^{n+1^{\#}}\Big]\leq 0. \tag{4.23}$$

Using Equations (4.18), the specific total energy may be written as $E_j^{k,n}=e(\tau_j^{k,n},S_j^{k,n})+(\eta_j^{k,n}-(\Pi_j^{k,n})^2)/2(a_j^n)^2$, so we have

$$\begin{aligned}
E_j^{k,n+1^{\#}}-E_j^{k,n} &= e(\tau_j^{k,n+1^{\#}},S_j^{k,n+1^{\#}})-e(\tau_j^{k,n},S_j^{k,n})+\frac{\eta_j^{k,n+1^{\#}}-\eta_j^{k,n}}{2(a_j^n)^2}\\
&\quad -\frac{(\Pi_j^{k,n+1^{\#}}-\Pi_j^{k,n})^2}{2(a_j^n)^2}-\frac{\Pi_j^{k,n}(\Pi_j^{k,n+1^{\#}}-\Pi_j^{k,n})}{(a_j^n)^2}.
\end{aligned}$$

Note that the operation (4.22d)$+(a_j^n)^2\times$(4.22a) leads to $\Pi_j^{k,n+1^{\#}}-\Pi_j^{k,n}=-(a_j^n)^2(\tau_j^{k,n+1^{\#}}-\tau_j^{k,n})$. Moreover, data at time $t^{(n)}$ are at equilibrium, thus $\Pi_j^{k,n}=\mathrm{p}(\tau_j^{k,n},S_j^{k,n})=-(\partial_\tau e)_{\mathrm{s}}(\tau_j^{k,n},S_j^{k,n})$. Further using (4.22c), we obtain

$$\begin{aligned}
&E_j^{k,n+1^{\#}}-E_j^{k,n}-\frac{\eta_j^{k,n+1^{\#}}-\eta_j^{k,n}}{2(a_j^n)^2}\\
&=e(\tau_j^{k,n+1^{\#}},S_j^{k,n})-e(\tau_j^{k,n},S_j^{k,n})
\end{aligned}$$

$$-(\partial_\tau e)_{\rm s}(\tau_j^{k,n},S_j^{k,n})(\tau_j^{k,n+1^\#}-\tau_j^{k,n})-\frac{(a_j^n)^2}{2}(\tau_j^{k,n+1^\#}-\tau_j^{k,n})^2.$$

Applying a second-order Taylor development with integral remainder of $e(\tau_j^{k,n+1^\#},S_j^{k,n})$ about $(\tau_j^{k,n},S_j^{k,n})$, we obtain

$$E_j^{k,n+1^\#}-E_j^{k,n}-\frac{\eta_j^{k,n+1^\#}-\eta_j^{k,n}}{2(a_j^n)^2}=(\tau_j^{k,n+1^\#}-\tau_j^{k,n})^2\times\cdots$$
$$\int_0^1\Big((\partial^2_{\tau\tau}e)_{\rm s}\big(\tau_j^{k,n}+\xi(\tau_j^{k,n+1^\#}-\tau_j^{k,n}),S_j^{k,n}\big)-(a_j^n)^2\Big)(1-\xi)d\xi.$$

Using the subcharacteristic condition (4.2), with $(\partial^2_{\tau\tau}e)_{\rm s}=-(\partial_\tau {\rm p})_{\rm s}$, the right-hand-side of the above equation is negative. Summing with the inequality (4.23), we get

$$E_j^{k,n+1^\#}-E_j^{k,n}-\lambda_k\tau_j^{k,n}\Big[\big\langle\Pi_h^{n+1^\#}u_h^{n+1^\#},d_x\phi_j^k\big\rangle_j^p-\delta_{k,p}H_{j+\frac12}^{n+1^\#}+\delta_{k,0}H_{j-\frac12}^{n+1^\#}\Big]\le 0.$$

We now go back to the discrete scheme (4.1) for the acoustic step whose component (4.1c) reads

$$E_j^{k,n+1^-}-E_j^{k,n}-\lambda_k\tau_j^{k,n}\Big[\big\langle\Pi_h^{n+1^-}u_h^{n+1^-},d_x\phi_j^k\big\rangle_j^p-\delta_{k,p}H_{j+\frac12}^{n+1^-}+\delta_{k,0}H_{j-\frac12}^{n+1^-}\Big]=0.$$

Setting $\tau_j^{k,n+1^\#}=\tau_j^{k,n+1^-}$, $U_j^{k,n+1^\#}=U_j^{k,n+1^-}$, and $\Pi_j^{k,n+1^\#}=\Pi_j^{k,n+1^-}$ implies $H_{j\pm\frac12}^{n+1^\#}=H_{j\pm\frac12}^{n+1^-}$. Subtracting the two above equations, we obtain $E_j^{k,n+1^\#}\le E_j^{k,n+1^-}$ while Equations (4.1a,b,d) are identical to Equations (4.22a,b,d).

As a consequence, $e_j^{k,n+1^\#}=e(\tau_j^{k,n+1^-},S_j^{k,n})\le e_j^{k,n+1^-}=e(\tau_j^{k,n+1^-},S_j^{k,n+1^-})$. Since from the inequality (4.15) $\tau_j^{k,n+1^-}>0$, we obtain $e_j^{k,n+1^-}\ge e_j^{k,n+1^\#}>0$. Moreover, from $(\partial_e {\rm s})_\tau>0$ we get $S_j^{k,n+1^-}\ge S_j^{k,n}$. ∎

THEOREM 4.1. *Assume $\mathbf{U}_{j\in\mathbb{Z}}^{0\le k\le p,n}$ are in Ω^a. Then under the CFL condition (4.14) and subcharacteristic condition (4.2), the LPDG scheme satisfies positivity for the mean value of the numerical solution:*

$$\overline{\rho}_j^{n+1}>0,\quad e(\overline{\mathbf{u}}_j^{n+1})>0 \tag{4.24}$$

and the discrete entropy inequality for $\mathcal{U}$ in the inequality (2.2):

$$\mathcal{U}(\overline{\mathbf{u}}_j^{n+1})-\overline{\mathcal{U}}_j^n+\lambda\big(u_{j+\frac12}^{\star,n+1^-}\widehat{\mathcal{U}}_{j+\frac12}^{n+1^-}-u_{j-\frac12}^{\star,n+1^-}\widehat{\mathcal{U}}_{j-\frac12}^{n+1^-}\big)\le 0, \tag{4.25}$$

with

$$\widehat{\mathcal{U}}_{j+\frac12}^{n+1^-}=-(u_{j+\frac12}^{\star,n+1^-})^+\rho S_j^{p,n+1^-}-(u_{j+\frac12}^{\star,n+1^-})^-\rho S_{j+1}^{0,n+1^-}. \tag{4.26}$$

Proof. From assumptions of Theorem 4.1, the results of Lemmas 4.1 and 4.3 hold. Positivity of the mean value of the density in the inequalities (4.24) thus follows from the convex combination (4.16) with $\rho_{j\in\mathbb{Z}}^{0\le k\le p,n+1^-}>0$. Likewise, the mapping $\mathbf{u}\mapsto\rho e(\mathbf{u})$ being concave, we also obtain $\overline{\rho}_j^{n+1}e(\overline{\mathbf{u}}_j^{n+1})>0$ from Equations (4.16) with $e_{j\in\mathbb{Z}}^{0\le k\le p,n+1^-}>0$.

Then, multiplying the second of the inequalities (4.20) with $\frac{\omega_k}{2} L_j^{k,n+1^-} \rho_j^{k,n+1^-} = \frac{\omega_k}{2} \rho_j^{k,n} > 0$ from Equation (4.6) and summing over $0 \le k \le p$ gives

$$\sum_{k=0}^{p} \frac{\omega_k}{2} \left(L_j^{k,n+1^-} \rho S_j^{k,n+1^-} - \rho S_j^{k,n} \right) = \sum_{k=0}^{p} \frac{\omega_k}{2} L_j^{k,n+1^-} \rho S_j^{k,n+1^-} - \overline{\rho S}_j^n \ge 0.$$

Now, using Equation (4.5) gives

$$\overline{\rho S}_j^{n+1^-} \ge \overline{\rho S}_j^n - \lambda \sum_{k=0}^{p} \rho S_j^{k,n+1^-} \left[- \left\langle u_h^{n+1^-}, d_x \phi_j^k \right\rangle_j^p + \delta_{k,p} u_{j+\frac{1}{2}}^{\star,n+1^-} - \delta_{k,0} u_{j-\frac{1}{2}}^{\star,n+1^-} \right].$$

Since $\mathbf{u} \mapsto \rho \mathrm{s}(\mathbf{u})$ is a concave function, Equation (4.16) induces

$$\begin{aligned} \rho \mathrm{s}(\overline{\mathbf{u}}_j^{n+1}) \ge \overline{\rho S}_j^{n+1^-} & \\ & - \lambda \sum_{k=0}^{p} \left(\left\langle u_h^{n+1^-}, d_x \phi_j^k \right\rangle_j^p - \delta_{k,p} (u_{j+\frac{1}{2}}^{\star,n+1^-})^- + \delta_{k,0} (u_{j-\frac{1}{2}}^{\star,n+1^-})^+ \right) \rho S_j^{k,n+1^-} \\ & - \lambda (u_{j+\frac{1}{2}}^{\star,n+1^-})^- \rho S_{j+1}^{0,n+1^-} + \lambda (u_{j-\frac{1}{2}}^{\star,n+1^-})^+ \rho S_{j-1}^{p,n+1^-} \end{aligned}$$

Summing the two last inequalities leads to the inequality (4.25) with $\mathcal{U} = -\rho \mathrm{s}$. ∎

Note that using the concavity of $\mathbf{u} \mapsto \rho \mathrm{s}(\mathbf{u})$ prevents the use of the same evaluation of entropy at times $t^{(n)}$ and $t^{(n+1)}$ in the inequality (4.25). As a consequence, the Lax–Wendroff theorem cannot be applied to prove convergence to an entropy solution, the limiter (4.29) is an attempt to circumvent this difficulty. We refer the reader to [2] and references therein for an in-depth discussion on discrete entropy inequalities for high-order schemes.

4.3. Analysis in the low Mach number regime. Explicit shock-capturing methods are known to experience temporal and spatial over-resolution issues in the low Mach number regime. In the following we apply a scale analysis of the discrete equations to evaluate the behavior of the method in this regime. Let l_∞, t_∞, ρ_∞, $u_\infty = l_\infty / t_\infty$, p_∞ and $e_\infty = u_\infty^2$ be the characteristic scales of the different variables in the Euler equations. Thermodynamic variables are linked through $\mathrm{p}_\infty = \rho_\infty c_\infty^2$, with c_∞ the characteristic sound speed, and we define $M_\infty = u_\infty / c_\infty$ the characteristic Mach number.

In the following, we will only consider the discrete equations in non-dimensional form by using the above scales. For the sake of simplicity, we keep the same notations for non-dimensional quantities without any possible confusion. In order to evalute the magnitude of the truncation error of the equations, we assume that the solution is smooth enough, $\mathbf{u}$ in $\mathcal{C}^{p+1}(\Omega, \mathbb{R}_+)$, and that the numerical solution satisfies $\mathbf{u}_h(x,t) = \mathbf{u}(x,t) + \mathcal{O}(h^{p+1}, \Delta t)$ in $\Omega \times \mathbb{R}_+$. Similar assumptions hold for $\mathbf{w}$ and $\mathbf{w}_h$. We further consider data at equilibrium (3.6) and assume a uniform numerical parameter, $a_{j \in \mathbb{Z}}^n = a$, without loss of generality.

Consider first the acoustic step (4.1) for the Lagrange variables. Equation $\frac{1}{\lambda_k} \times$(4.1b) in non-dimensional form reads

$$\begin{aligned} \frac{\omega_k h}{2} \frac{U_j^{k,n+1^-} - U_j^{k,n}}{\Delta t} + \frac{\tau_j^{k,n}}{M_\infty^2} \Big[\left\langle \partial_x \Pi_h^{n+1^-}, \phi_j^k \right\rangle_j^p & + \delta_{k,p} (\Pi_{j+\frac{1}{2}}^{\star,n+1^-} - \Pi_j^{p,n+1^-}) \\ & - \delta_{k,0} (\Pi_{j-\frac{1}{2}}^{\star,n+1^-} - \Pi_j^{0,n+1^-}) \Big] = 0. \end{aligned}$$

Summing the contributions over $0 \le k \le p$, the two first terms read

$$\sum_{k=0}^{p} \frac{\omega_k h}{2} \Big(\frac{U_j^{k,n+1^-} - U_j^{k,n}}{\Delta t} + \frac{\tau_j^{k,n}}{M_\infty^2} \partial_x \Pi_h^{n+1^-} \Big) \phi_j^k = \int_\kappa \partial_t u^n + \frac{\tau^n}{M_\infty^2} \partial_x \mathrm{p}^n dx + h\mathcal{O}(h^p, \Delta t),$$

where we have assumed that $\partial_x \mathrm{p} = \mathcal{O}(M_\infty^2)$ to ensure that both terms $\partial_t u$ and $\tau \partial_x \mathrm{p}$ have the same magnitude in the limit $M_\infty \ll 1$.

The non-dimensional numerical fluxes read

$$u_{j+\frac{1}{2}}^{\star,n+1^-} = \frac{U_j^{p,n+1^-} + U_{j+1}^{0,n+1^-}}{2} + \frac{1}{M_\infty} \frac{\Pi_j^{p,n+1^-} - \Pi_{j+1}^{0,n+1^-}}{2a}, \tag{4.27a}$$

$$\Pi_{j+\frac{1}{2}}^{\star,n+1^-} = \frac{\Pi_j^{p,n+1^-} + \Pi_{j+1}^{0,n+1^-}}{2} + M_\infty \frac{a(U_j^{p,n+1^-} - U_{j+1}^{0,n+1^-})}{2}, \tag{4.27b}$$

and lead to $\Pi_{j+\frac{1}{2}}^{\star,n+1^-} - \Pi_j^{p,n+1^-} = \mathcal{O}(M_\infty h^{p+1})$. Summing all contributions, one obtains that the mean value in cell of (4.1b) is consistent with

$$\frac{1}{h} \int_\kappa \partial_t u^n + \tau^n \partial_x \mathrm{p}^n dx + \mathcal{O}(\tfrac{h^p}{M_\infty}, \Delta t),$$

where the leading error in space follows from the dissipation term in the numerical flux $\Pi_{j+\frac{1}{2}}^{\star,n+1^-}$ and will polute the numerical solution in the limit $M_\infty \ll 1$. Accuracy requirements will thus lead to over-resolution in space. We refer to [6] for an in-depth scale analysis of the truncation error in the context of LP like schemes.

Using an explicit time discretization would also lead to over-resolution in time since the time step will be limited by the acoustic waves $|u| + c/M_\infty$ from the CFL condition. We relax this limitation by using an implicit time discretization of the acoustic terms and the CFL condition (4.14) in non-dimensional form remains unchanged.

However, the time implicit discretization of the acoustic step requires the solution of a linear system for the Lagrange variables $\mathbf{W}_{j\in\mathbb{Z}}^{0\le k\le p,n+1^-}$ at each time step. Solving Equations (4.1b,d) for the velocity and relaxation pressure will lead to issues in the linear system inversion when $M_\infty \ll 1$ because of the above mentioned dissipation amplification and the fact that both equations have different scales: u_∞ for Equation (4.1b) must be compared to $\mathrm{p}_\infty/(\rho_\infty c_\infty)$ for Equation (4.1d) which leads to a ratio M_∞. Considering the characteristic variables (4.11) allows to circumvent those difficulties since both Equations (4.11a,d) that need to be inverted have the same magnitude. Moreover, the non-dimensional transport Equation (4.11a) for $\overrightarrow{w}_h = \Pi_h + M_\infty a u_h$ reads

$$\frac{\omega_k h}{2} \frac{\overrightarrow{W}_j^{k,n+1^-} - \overrightarrow{W}_j^{k,n}}{\Delta t} + \frac{a\tau_j^{k,n}}{M_\infty} \Big[\big\langle \partial_x \overrightarrow{w}_h^{n+1^-}, \phi_j^k \big\rangle_j^p - \delta_{k,0} \big(\overrightarrow{W}_{j-1}^{p,n+1^-} - \overrightarrow{W}_j^{0,n+1^-} \big) \Big],$$

so the mean value in cell of Equation (4.11a) is consistent with

$$\frac{1}{h} \int_\kappa \partial_t \overrightarrow{w}^n + \tfrac{a\tau^n}{M_\infty} \partial_x \overrightarrow{w}^n \, dx + \mathcal{O}(h^p, \Delta t),$$

where we have used the fact that $\partial_x \overrightarrow{w} = \mathcal{O}(M_\infty)$. A similar results holds for Equation (4.11d) which means that the conditioning of the linear system (4.11a,d) is not affected in the limit $M_\infty \ll 1$.

Finally, note that the non-dimensional Equations (4.3) for the transport step remain unchanged for all variables and are not affected in the low Mach number regime since $u_{j+\frac{1}{2}}^{\star,n+1^-} = u(x_{j+\frac{1}{2}}, t^n) + \mathcal{O}(h^{p+1}, \Delta t)$ from Equation (4.27a).

4.4. Limiting strategy. We now apply limiters to extend the properties of Theorem 4.1 from the mean value of the solution to nodal values at interpolation points within elements. We use the strategy introduced in [22], based on limiters derived in [31,32], that we extend to positivity of the internal energy.

First, we enforce positivity at nodal values of density and internal energy through the modifications

$$\breve{\rho}_j^{k,n+1} = \theta_j^{\rho}(\rho_j^{k,n+1} - \overline{\rho}_j^{n+1}) + \overline{\rho}_j^{n+1}, \tag{4.28a}$$

$$\ddot{\mathbf{U}}_j^{k,n+1} = \theta_j^{e}(\breve{\mathbf{U}}_j^{k,n+1} - \overline{\mathbf{u}}_j^{n+1}) + \overline{\mathbf{u}}_j^{n+1}, \tag{4.28b}$$

with $\breve{\mathbf{U}}_j^{k,n+1} = (\breve{\rho}_j^{k,n+1}, \rho U_j^{k,n+1}, \rho E_j^{k,n+1})^{\top}$ and where $0 \le \theta_j^{\rho}, \theta_j^{e} \le 1$ are defined by

$$\theta_j^{\rho} = \min\Big(\frac{\overline{\rho}_j^n - \epsilon}{\overline{\rho}_j^n - \rho_j^{min}}, 1\Big), \quad \rho_j^{min} = \min_{0\le k\le p} \rho_j^{k,n+1},$$

$$\theta_j^{e} = \min_{0\le k\le p}\Big(\theta_j^{e,k} : \quad e\big(\theta_j^{e,k}(\breve{\mathbf{U}}_j^{k,n+1} - \overline{\mathbf{u}}_j^{n+1}) + \overline{\mathbf{u}}_j^{n+1}\big) \ge \epsilon\Big),$$

and $0 < \epsilon \ll 1$ is a parameter.

Then, we strengthen the entropy inequality (4.25) by observing that the discrete transport step (4.3) satisfies

$$\mathcal{U}(\overline{\mathbf{u}}_j^{n+1}) \le \mathcal{U}_j^{n+1^-} := \max\big(\mathcal{U}(\mathbf{U}_{j-1}^{p,n+1^-}), \mathcal{U}(\mathbf{U}_j^{0\le k\le p,n+1^-}), \mathcal{U}(\mathbf{U}_{j+1}^{0,n+1^-})\big).$$

We thus impose a maximum principle at nodal values with

$$\tilde{\mathbf{U}}_j^{k,n+1} = \theta_j^{s}(\ddot{\mathbf{U}}_j^{k,n+1} - \overline{\mathbf{u}}_j^{n+1}) + \overline{\mathbf{u}}_j^{n+1}, \tag{4.29}$$

where $0 \le \theta_j^{s} \le 1$ is defined by

$$\theta_j^{s} = \min_{0\le k\le p}\Big(\theta_j^{s,k} : \mathcal{U}\big(\theta_j^{s,k}(\ddot{\mathbf{U}}_j^{k,n+1} - \overline{\mathbf{u}}_j^{n+1}) + \overline{\mathbf{u}}_j^{n+1}\big) = \mathcal{U}_j^{n+1^-}\Big).$$

The DOFs at time $t^{(n+1)}$ are then replaced by the limited values $\tilde{\mathbf{U}}_{j\in\mathbb{Z}}^{0\le k\le p,n+1}$. We stress that limiters (4.28) and (4.29) keep the mean value of conservative variables and are therefore conservative.

5. Numerical experiments

In this section we present several numerical experiments to illustrate the performances of the LPDG scheme derived in this work. For all experiments, we consider a polytropic ideal gas with an equation of state of the form $\mathrm{p}(\tau,\mathrm{s}) = (\gamma-1)\frac{e(\tau,\mathrm{s})}{\tau}$ with $\gamma = 1.4$.

As proposed in [22], the present method is extended to high-order time integration by using strong-stability preserving explicit Runge–Kutta methods [26,27]. These methods consist in convex combinations of first-order forward Euler methods and thus will keep positivity of Theorem 4.1 under a given CFL condition. We use a Runge–Kutta scheme of order $p+1$ when using polynomials of degree p for the space discretization: the two-stage second-order Heun method for $p=1$, the three-stage third-order scheme of Shu and Osher [26] for $p=2$, and the five-stage fourth-order scheme of Spiteri and Ruuth [27] for $p=3$, respectively.

Our strategy at the discrete level consists in the following algorithm applied at each stage of the Runge–Kutta method:

(1) solve the linear system (4.11) with data at equilibrium (4.4a);
(2) compute the discrete residuals of the LPDG scheme (4.7) with the values (4.4b) and advance in time;
(3) apply the limiters (4.28) and (4.29).

Finally, the *a priori* CFL condition (4.14) and subcharacteristic condition (4.2) are imposed at time $t^{(n)}$ as was proposed in [6,10] for the computation of the time step and numerical dissipation parameter:

$$\Delta t = CFL \min_{j\in\mathbb{Z}} \min_{0\le k\le p} \frac{\omega_k h}{2\big(\langle u_h^n, d_x\phi_j^k\rangle_j^p - \delta_{k,p}(u_{j+\frac12}^{\star,n})^- + \delta_{k,0}(u_{j-\frac12}^{\star,n})^+\big)}, \tag{5.1a}$$

$$a_j^n = k_{AD} \max_{0\le k\le p} \sqrt{-\partial_\tau \mathrm{p}\big(\tau_j^{k,n}, S_j^{k,n}\big)}, \tag{5.1b}$$

with $0<CFL<1$ and $k_{AD}>1$ to satisfy the strict inequalities (4.14) and (4.2). The numerical experiments in the following have been obtained with $CFL=0.95$ and $k_{AD}=1.05$ unless stated otherwise.

p	h	$\|e_h\|_{L^1(\Omega)}$	$\mathcal{O}_1$	$\|e_h\|_{L^2(\Omega)}$	$\mathcal{O}_2$	$\|e_h\|_{L_\infty(\Omega)}$	$\mathcal{O}_\infty$
	1/4	0.10181e+00	–	0.14232e+00	–	0.20163e+00	–
	1/8	0.14351e+00	−0.50	0.15579e+00	−0.13	0.21436e+00	−0.09
1	1/16	0.66130e−01	1.12	0.73104e−01	1.09	0.10431e+00	1.04
	1/32	0.18838e−01	1.81	0.20925e−01	1.80	0.29770e−01	1.81
	1/64	0.48321e−02	1.96	0.53656e−02	1.96	0.75967e−02	1.97
	1/4	0.36351e−01	–	0.45015e−01	–	0.67931e−01	–
	1/8	0.30861e−02	3.56	0.37171e−02	3.60	0.59017e−02	3.52
2	1/16	0.24518e−03	3.65	0.28065e−03	3.73	0.44376e−03	3.73
	1/32	0.22609e−04	3.44	0.25508e−04	3.46	0.43346e−04	3.36
	1/64	0.23418e−05	3.27	0.28046e−05	3.19	0.67006e−05	2.69
	1/4	0.10125e−02	–	0.11690e−02	–	0.21883e−02	–
	1/8	0.40099e−04	4.66	0.55908e−04	4.39	0.19290e−03	3.50
3	1/16	0.23112e−05	4.12	0.34132e−05	4.03	0.12993e−04	3.89
	1/32	0.14242e−06	4.02	0.21316e−06	4.00	0.82283e−06	3.98
	1/64	0.88743e−08	4.00	0.13324e−07	4.00	0.51564e−07	4.00
	1/4	0.12450e−02	–	0.13193e−02	–	0.27464e−02	–
	1/8	0.56690e−04	4.46	0.76725e−04	4.10	0.25787e−03	3.41
$3^\star$	1/16	0.57115e−05	3.31	0.71739e−05	3.42	0.21680e−04	3.57
	1/32	0.70874e−06	3.01	0.81522e−06	3.14	0.19312e−05	3.49
	1/64	0.88552e−07	3.00	0.99248e−07	3.04	0.19058e−06	3.34

TABLE 5.1. *Density wave problem with $M_\infty=5\times10^{-1}$: different norms of the error at time $t=5$ and associated orders of convergence. The star symbol indicates that the computation has been obtained by using a Runge–Kutta method of order p instead of $p+1$.*

5.1. Convection of a density wave. We first consider the convection of a density wave in a uniform flow with Mach number M_∞. Let $\Omega=(0,1)$. We solve the

p	h	$\|e_h\|_{L^1(\Omega)}$	$\mathcal{O}_1$	$\|e_h\|_{L^2(\Omega)}$	$\mathcal{O}_2$	$\|e_h\|_{L_\infty(\Omega)}$	$\mathcal{O}_\infty$
	1/4	0.10181e+00	–	0.14232e+00	–	0.20163e+00	–
	1/8	0.14351e+00	−0.50	0.15579e+00	−0.13	0.21436e+00	−0.09
1	1/16	0.66130e−01	1.12	0.73104e−01	1.09	0.10431e+00	1.04
	1/32	0.18838e−01	1.81	0.20925e−01	1.80	0.29770e−01	1.81
	1/64	0.48321e−02	1.96	0.53656e−02	1.96	0.75967e−02	1.97
	1/4	0.36351e−01	–	0.45015e−01	–	0.67931e−01	–
	1/8	0.30861e−02	3.56	0.37171e−02	3.60	0.59017e−02	3.52
2	1/16	0.24518e−03	3.65	0.28065e−03	3.73	0.44376e−03	3.73
	1/32	0.22609e−04	3.44	0.25508e−04	3.46	0.43346e−04	3.36
	1/64	0.23418e−05	3.27	0.28046e−05	3.19	0.67006e−05	2.69
	1/4	0.10125e−02	–	0.11690e−02	–	0.21883e−02	–
	1/8	0.40099e−04	4.66	0.55908e−04	4.39	0.19290e−03	3.50
3	1/16	0.23112e−05	4.12	0.34132e−05	4.03	0.12993e−04	3.89
	1/32	0.14242e−06	4.02	0.21316e−06	4.00	0.82283e−06	3.98
	1/64	0.89125e−08	4.00	0.13347e−07	4.00	0.51587e−07	4.00

TABLE 5.2. *Density wave problem with $M_\infty = 5\times10^{-3}$: different norms of the error at time $t=5$ and associated orders of convergence.*

problem	left state $(\rho_L, u_L, \mathrm{p}_L)^\top$	right state $(\rho_R, u_R, \mathrm{p}_R)^\top$	x_0
Sod	$(1,0,1)^\top$	$(0.125,0,0.1)^\top$	0
Lax	$(0.445,0.698,3.528)^\top$	$(0.5,0,0.571)^\top$	0
Toro 2	$(1,-2,0.4)^\top$	$(1,2,0.4)^\top$	0
Toro 4	$(5.99924,19.5975,460.894)^\top$	$(5.99242,-6.19633,46.0950)^\top$	−0.1

TABLE 5.3. *Initial conditions of Riemann problems.*

problem (2.1) with periodicity conditions and the initial condition

$$\rho_0(x) = 1 + 0.2\sin(2\pi x), \quad u_0(x) = 1, \quad \mathrm{p}_0(x) = \frac{1}{\gamma M_\infty^2}, \quad \forall x \in \Omega.$$

Tables 5.1 and 5.2 indicate for two Mach number values the norms of the numerical error on density $e_h = \rho_h - \rho$ for different polynomial degrees and grid refinements with associated convergence orders in space. The expected $p+1$ order of convergence is recovered with the present method. Moreover, in Table 5.1 the $p=3$ computations are associated to either a fourth-order or a third-order Runge–Kutta method. We observe that the error levels are limited by the accuracy of the time integration which indicates that, in practice, the proposed strategy for the time integration keeps the theoretical accuracy of the Runge–Kutta scheme.

Comparing results in Tables 5.1 and 5.2 we note that the error values are almost identical, so the scheme accuracy is insensitive to the Mach number, while the time step from (4.14) is independent of the acoustic wave speed. The LPDG scheme thus seems to be well adapted for the simulation of low Mach number flows in agreement with the theoretical analysis in Section 4.3.

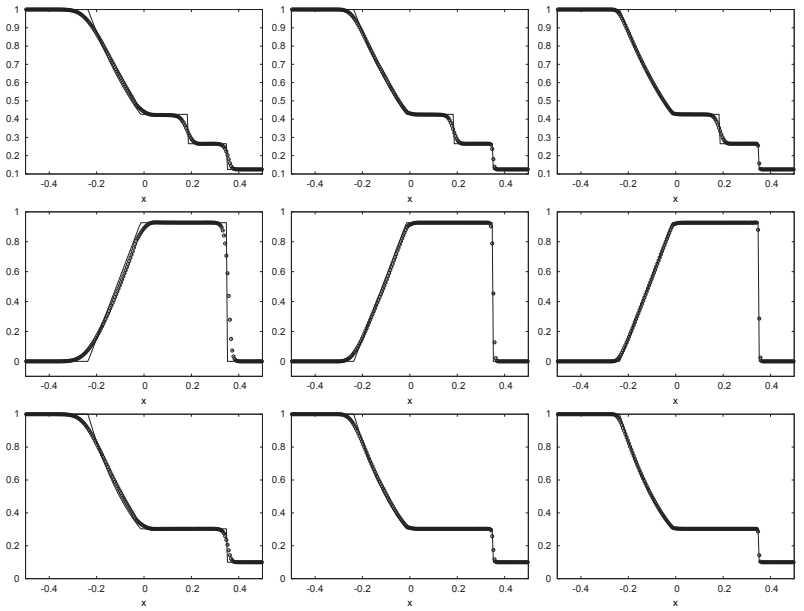

(a) $p=1$ (b) $p=2$ (c) $p=3$

FIG. 5.1. *Sod problem: numerical solution (symbols) for density (top), velocity (middle) and pressure (bottom) at time* $t=0.2$ *for polynomial degrees* $1\leq p\leq 3$ *and* $h=\frac{1}{200}$.

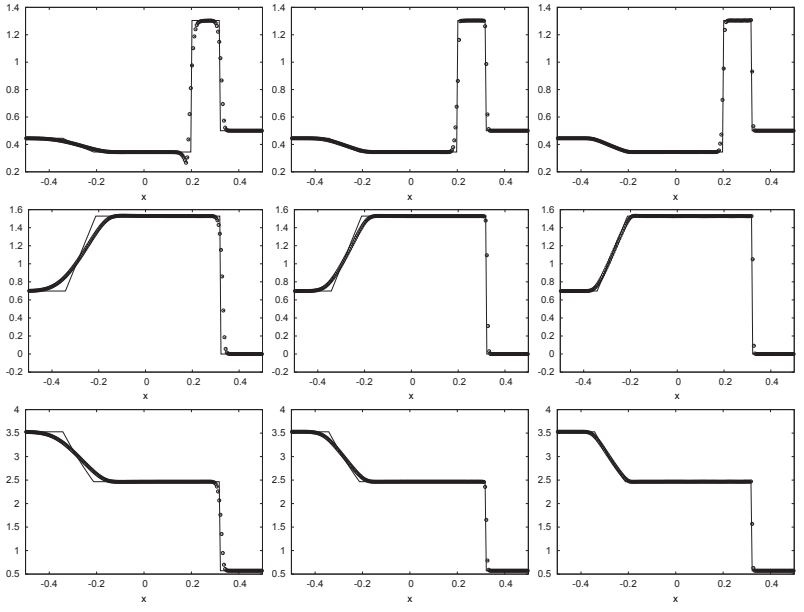

(a) $p=1$ (b) $p=2$ (c) $p=3$

FIG. 5.2. *Lax problem: numerical solution (symbols) for density (top), velocity (middle) and pressure (bottom) at time* $t=0.13$ *for polynomial degrees* $1\leq p\leq 3$ *and* $h=\frac{1}{200}$.

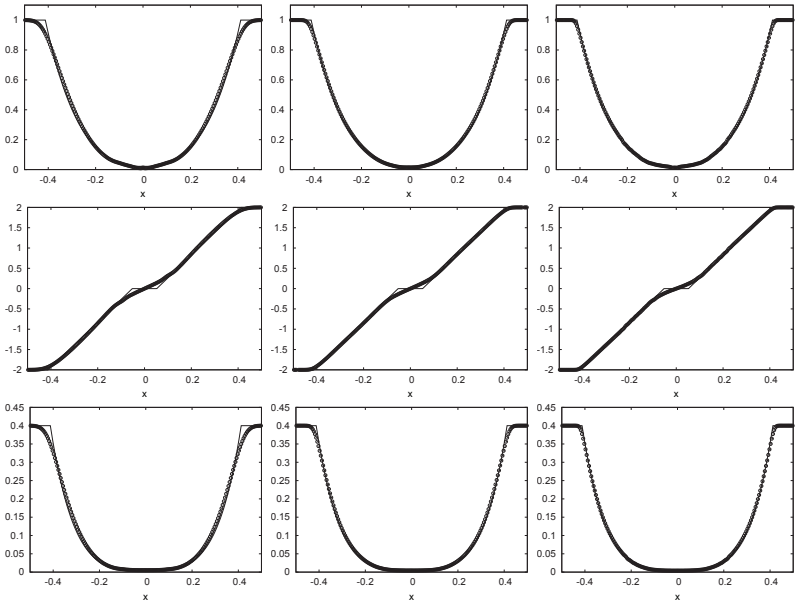

(a) $p=1$ (b) $p=2$ (c) $p=3$

FIG. 5.3. *Toro problem 2: numerical solution (symbols) for density (top), velocity (middle) and pressure (bottom) at time* $t=0.15$ *for polynomial degrees* $1\leq p\leq 3$ *and* $h=\frac{1}{200}$.

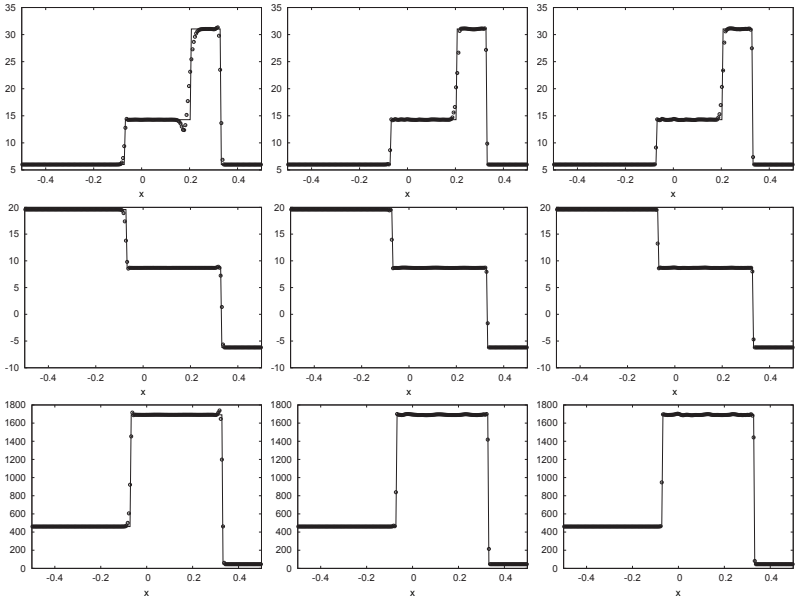

(a) $p=1$ (b) $p=2$ (c) $p=3$

FIG. 5.4. *Toro problem 4: numerical solution (symbols) for density (top), velocity (middle) and pressure (bottom) at time* $t=0.035$ *for polynomial degrees* $1\leq p\leq 3$ *and* $h=\frac{1}{200}$.

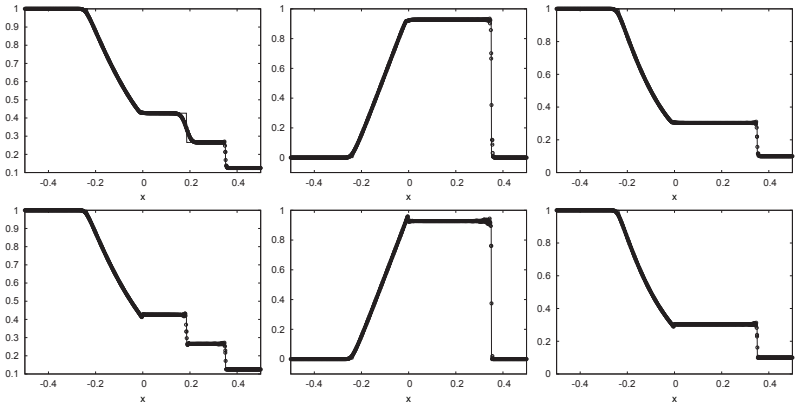

(a) density (b) velocity (c) pressure

FIG. 5.5. *Sod problem: numerical solution at interpolation points (symbols) at time* $t=0.2$ *for* $p=3$ *and* $h=\frac{1}{200}$ *with (top) and without (bottom) limiters.*

5.2. Riemann problems. We now consider the Riemann problems given in Table 5.3 with initial condition $\mathbf{u}_0(x)=\mathbf{u}_L$ if $x<x_0$ or $\mathbf{u}_0(x)=\mathbf{u}_R$ if $x>x_0$. Toro problems are taken from [28]. Figures 5.1 to 5.5 compare the numerical solution in symbols with the exact solution in lines.

For Sod and Lax problems, results are qualitatively similar. The shock waves are well captured and the increase in the discretization order has a clear positive effect on the approximation of the rarefaction and contact waves. Similar conclusions are drawn from the Toro problem 4, but some spurious oscillations of low amplitude are visible in the neighborhood of strong shocks with the highest discretization order $p=3$. Note that larger oscillations have been effectively damped by increasing the numerical dissipation with $k_{AD}=1.2$ in Equation (5.1b). The solution for the Toro problem 2 is made of two symmetric rarefaction waves with formation of near-vacuum in the intermediate region. The positivity limiter (4.28) is successful to keep robustness of the computation and increasing p reduces the diffusion at the tail of the waves as expected.

Figure 5.5 illustrates the effect of the limiters (4.28) and (4.29) on the quality of the solution. The internal structure of the numerical solution is shown by plotting the solution at $p+1$ interpolation points within each element for the Sod problem and a fourth-order scheme. Some low amplitude spurious oscillations appear in the solution without limiters but keep sharp resolution of all waves. The limiters allow one to keep a monotone evolution of the solution around discontinuities, but the entropy limiter (4.29) smears out the contact discontinuity.

6. Concluding remarks

In this work, a high-order extension with a DG method [22] of LP like schemes [10] is adapted to the compressible Euler equations with a general equation of state. Moreover, the numerical dissipation is tuned with a local parameter thus allowing one to introduce only the artificial dissipation needed at the elementwise level.

Using a DG method of arbitrary order for the space discretization associated to a first-order implicit-explicit time discretization of acoustic and transport operators, *a priori* conditions on the time step and on the numerical parameter imposing the subcharacteristic condition are derived in order to guaranty positivity of the mean value

in each mesh element of density and internal energy, as well as to satisfy a discrete inequality for the physical entropy. *A posteriori* limiters [31,32] are then used to extend these properties to nodal values within elements. Strong-stability preserving Runge–Kutta schemes are applied for the time integration in order to keep positivity at any time discretization order.

Numerical experiments in one space dimension highlight high-order approximation of smooth solutions, while the method proves to be robust in the presence of discontinuities or vacuum. Large time steps are allowed while keeping accuracy on smooth solutions even for low Mach number flows. Future investigations will consider the conditions to conserve the properties of the numerical scheme with a formally high-order time discretization and the extension to several space dimensions.

Acknowledgments. Frédéric Coquel from École Polytechnique is warmly acknowledged for its fruitful comments and encouragement at numerous stages of this work.

REFERENCES

[1] C. Berthon, *Robustness of MUSCL schemes for 2D unstructured meshes*, J. Comput. Phys., 218:495–509, 2006.

[2] C. Berthon and V. Desveaux, *An entropy preserving MOOD scheme for the Euler equations*, Int. J. Finite Volumes, 11:1–39, 2014.

[3] F. Bouchut, *Nonlinear Stability of Finite Volume Methods for Hyperbolic Conservation Laws and Well-Balanced Schemes for Sources*, Birkhauser, 2004.

[4] C. Chalons and F. Coquel, *Navier–Stokes equations with several independent pressure laws and explicit predictor-corrector schemes*, Numer. Math., 101:451–478, 2005.

[5] C. Chalons and J.F. Coulombel, *Relaxation approximation of the Euler equations*, J. Math. Anal. Appl., 348:872–893, 2008.

[6] C. Chalons, M. Girardin, and S. Kokh, *Large time step and asymptotic preserving numerical schemes for the gas dynamics equations with source terms*, SIAM J. Sci. Comput., 35:A2874–A2902, 2013.

[7] B. Cockburn and C.W. Shu, *TVB Runge–Kutta local projection discontinuous Galerkin finite element method for scalar conservation laws II: general framework*, Math. Comput., 52:411–435, 1989.

[8] B. Cockburn and C.W. Shu, *Runge–Kutta discontinuous Galerkin methods for convection-dominated problems*, J. Sci. Comput., 16:173–261, 2001.

[9] F. Coquel, E. Godlewski, A. In, B. Perthame, and P. Rascle, *Some new Godunov and relaxation methods for two-phase flow problems*, in Godunov Methods, Kluwer/Plenum, New York, 2001.

[10] F. Coquel, Q. Long-Nguyen, M. Postel, and Q.H. Tran, *Entropy-satisfying relaxation method with large time-steps for Euler IBVPs*, Math. Comput., 79:1493–1533, 2010.

[11] B. Després, *Entropy inequality for high order discontinuous Galerkin approximation of Euler equations*, in VII Conference on Hyperbolic Problems, ETHZ-Zurich, 1998.

[12] B. Després, *Discontinuous Galerkin method for the numerical solution of Euler equations in axisymmetric geometry*, in Discontinuous Galerkin Methods: Theory, Computation and Applications, Springer–Verlag, 2000.

[13] S. Jin and Z.P. Xin, *The relaxation schemes for systems of conservation laws in arbitrary space dimension*, Comm. Pure Appl. Math., 48:235–276, 1995.

[14] N. Kroll, H. Bieler, H. Deconinck, V. Couaillier, H. van der Ven and K. Sorensen (eds.), *ADIGMA - A European initiative on the development of adaptive higher-order variational methods for aerospace applications*, in Notes on Numerical Fluid Mechanics and Multidisciplinary Design, Springer Verlag, 2010.

[15] E. Godlewski and P.-A. Raviart, *Numerical Approximation of Hyperbolic Systems of Conservation Laws*, Springer–Verlag, New York, 1996.

[16] D.A. Kopriva and G. Gassner, *On the quadrature and weak form choices in collocation type discontinuous Galerkin spectral element methods*, J. Sci. Comput., 44:136–155, 2010.

[17] P. Lesaint and P.-A. Raviart, *On a finite element method for solving the neutron transport equation*, in Mathematical Aspects of Finite Elements in Partial Differential Equations, Academic

Press, New York, 1974.
[18] W.H. Reed and T.R. Hill, *Triangular mesh methods for the neutron transport equation*, Technical Report LA-UR-73-479, Los Alamos Scientific Laboratory, NM, 1973.
[19] B. Perthame and C.-W. Shu, *On positivity preserving finite volume schemes for Euler equations*, Numer. Math., 73:119–130, 1996.
[20] J. Qiu, B.C. Khoo and C.-W. Shu, *A numerical study for the performance of the Runge–Kutta discontinous Galerkin method based on different numerical fluxes*, J. Comput. Phys., 26:540–565, 2006.
[21] F. Renac, *Stationary discrete shock profiles for scalar conservation laws with a discontinuous Galerkin method*, SIAM J. Numer. Anal., 53:1690–1715, 2015.
[22] F. Renac, *A robust high-order Lagrange-projection like scheme with large time steps for the isentropic Euler equations*, Numer. Math., 135:493–519, 2017.
[23] F. Renac, M. de la Llave Plata, E. Martin, J.-B. Chapelier, and V. Couaillier, *Aghora: A high-order DG solver for turbulent flow simulations*, in IDIHOM: Industrialization of High-Order Methods — A Top-Down Approach, Springer–Verlag, 2015.
[24] F. Renac, S. Gérald, C. Marmignon, and F. Coquel, *Fast time implicit-explicit discontinuous Galerkin method for the compressible Navier–Stokes equations*, J. Comput. Phys., 251:272–291, 2013.
[25] F. Renac, C. Marmignon, and F. Coquel, *Time implicit high-order discontinuous Galerkin method with reduced evaluation cost*, SIAM J. Sci. Comput., 34:370–394, 2012.
[26] C.-W. Shu and S. Osher, *Efficient implementation of essentially non-oscillatory shock-capturing schemes*, J. Comput. Phys., 77:439–471, 1988.
[27] R.J. Spiteri and S.J. Ruuth, *A new class of optimal high-order strong-stability-preserving time discretization methods*, SIAM J. Numer. Anal., 40:469–491, 2002.
[28] E.F. Toro, *Riemann Solvers and Numerical Methods for Fluid Dynamics: A Practical Introduction*, Third Edition, Springer–Verlag, Berlin Heidelberg, 2009.
[29] F. Vilar, *Cell-centered discontinuous Galerkin discretization for two-dimensional Lagrangian hydrodynamics*, Comput. Fluids, 64:64–73, 2012.
[30] F. Vilar, P.-H. Maire, and R. Abgrall, *A discontinuous Galerkin discretization for solving the two-dimensional gas dynamics equations written under total Lagrangian formulation on general unstructured grids*, J. Comput. Phys., 276:188–234, 2014.
[31] X. Zhang and C.-W. Shu, *On maximum-principle-satisfying high order schemes for scalar conservation laws*, J. Comput. Phys., 229:3091–3120, 2010.
[32] X. Zhang and C.-W. Shu, *On positivity-preserving high order discontinuous Galerkin schemes for compressible Euler equations on rectangular meshes*, J. Comput. Phys., 229:8918–8934, 2010.